UNCLASSIFIED

AD 259 922

Reproduced by the

ARMED SERVICES TECHNICAL INFORMATION AGENCY
ARLINGTON HALL STATION
ARLINGTON 12, VIRGINIA

UNCLASSIFIED

BEST
AVAILABLE COPY

NOTICE: When government or other drawings, specifications or other data are used for any purpose other than in connection with a definitely related government procurement operation, the U. S. Government thereby incurs no responsibility, nor any obligation whatsoever; and the fact that the Government may have formulated, furnished, or in any way supplied the said drawings, specifications, or other data is not to be regarded by implication or otherwise as in any manner licensing the holder or any other person or corporation, or conveying any rights or permission to manufacture, use or sell any patented invention that may in any way be related thereto.

61-3-6
XEROX

AD 259022

ZPh-026
Physics Section

CATALOGED BY ASTIA
AS AD No. _____

INFRARED EMISSIVITY OF DIATOMIC GASES

FOR

THE ANHARMONIC VIBRATING ROTATOR MODEL

W. Malkmus
A. Thomson

May 5, 1961

This work was conducted under Contract No. AF19(604)-5554, ARPA Order No. 116, Project Defender.

ASTIA
RECEIVED
JUL 24 1961
TIPDR

CONVAIR SAN DIEGO CONVAIR DIVISION GENERAL DYNAMICS CORPORATION

ZPh-095
Physics Section

INFRARED EMISSIVITY OF DIATOMIC GASES

FOR

THE ANHARMONIC VIBRATING ROTATOR MODEL

W. Malkmus
A. Thomson

May 5, 1961

This work was conducted under Contract

No. AF19(604)-5554, ARPA Order No. 116,

Project Defender.

GENERAL DYNAMICS
CONVAIR SAN DIEGO
Convair Division of General Dynamics Corporation

CONTENTS

ILLUSTRATIONS

ILLUSTRATIONS

ILLUSTRATIONS

INFRARED EMISSIVITY OF DIATOMIC GASES FOR THE ANHARMONIC VIBRATING ROTATOR MODEL

W. Malkmus
A. Thomson

ABSTRACT

In order to compute the emissivity of a diatomic gas, a simplified model of a diatomic molecule is assumed: an anharmonic oscillator with the first approximation to the vibration-rotation interaction. For a given band, the frequency of emitted radiation is expressed as a quadratic function of the quantum number m, which is solved to express m as a function of ω. This expression is substituted for m in the equations used for computing the average line intensity and average line spacing. By applying the random Elsasser model to the fundamental and superposed higher order bands, closed-form solutions are obtained for the emissivity as a function of ω for certain limiting cases. Experimental data, where available, are used for the line widths and total absorption of the bands. The harmonic oscillator approximation is used to estimate strengths of higher order bands for which experimental data are not available. This analysis is applied to HCl, HF, CO, and NO for temperatures ranging from 300 to 7000°K.

I. INTRODUCTION

A first approximation to the infrared spectral emissivity of a diatomic gas can be made by assuming a harmonic oscillator model for the molecule.[8,9] This has the advantage of simplicity, but the very nearly symmetric intensity distribution which it yields does not closely match the asymmetric shape which is found experimentally or calculated by a line-by-line method.[1]

Tc improve the approximation, the model is assumed to be an anharmonic oscillator with the first approximation to the vibration-rotation interaction. This will improve the approximation to the actual spectral emissivity without resort to the more detailed approach of considering the emission from each individual spectral line.

II. DEVELOPMENT

The energy levels of an anharmonic oscillator, in the first approximation to the vibration-rotation interaction, are given by

$$E(v,j) = \omega_e \left(v + \frac{1}{2}\right) - \omega_e x_e \left(v + \frac{1}{2}\right)^2 + \omega_e y_e \left(v + \frac{1}{2}\right)^3 + \omega_e z_e \left(v + \frac{1}{2}\right)^4 + B_e j(j+1) - \alpha_e \left(v + \frac{1}{2}\right) j(j+1). \quad (1)$$

(Refer to the treatment of Stull and Plass[1] for notation and basic equations.) The frequency of a transition for $|\Delta v| = 1$ is then given by

$$\begin{aligned} \omega &= E(v+1, j') - E(v,j) \\ &= \omega_v + B_e[j'(j'+1) - j(j+1)] \\ &\quad - \alpha_e\left[\left(v + \frac{3}{2}\right) j'(j'+1) - \left(v + \frac{1}{2}\right) j(j+1)\right], \end{aligned} \quad (2)$$

where

$$\omega_v = \omega_e - 2(v+1)\,\omega_e x_e + \left[3(v+1)^2 + \frac{1}{4}\right] \omega_e y_e + \left[4(v+1)^3 + (v+1)\right] \omega_e z_e. \quad (3)$$

In terms of m($m = j + 1$ for the R-branch, $m = -j$ for the P-branch),

$$\omega = \omega_v + 2B_e m - \alpha_e[m(m+1) + 2\left(v + \tfrac{1}{2}\right) m]. \quad (4)$$

This equation expresses ω as a quadratic function of m. On solving for m, this becomes

$$m = \frac{B_e - \alpha_e(v+1) \mp \sqrt{[B_e - \alpha_e(v+1)]^2 - \alpha_e(\omega - \omega_v)}}{\alpha_e}. \quad (5)$$

Note that Equation (4) implies a maximum value for ω of

$$\omega_{max} = \omega_v + \frac{[B_e - \alpha_e(v + 1)]^2}{\alpha_e} \tag{6}$$

for

$$m = \frac{B_e - \alpha_e(v + 1)}{\alpha_e} \quad . \tag{7}$$

Since $[B_e - \alpha_e(v + 1)]/\alpha_e > o$ for all molecules under consideration, this model will always have a band head in the R-branch. Hence, the upper sign before the radical in Equation (5) refers to the main portion of the band and the lower sign to the returning R-branch. (This convention for the $\mp$ or $\pm$ sign will be used throughout this analysis.)

The average line spacing in the region of a given m is

$$d = 2|B_e - \alpha_e(v + 1 + m)|. \tag{8}$$

This becomes [expressed in terms of ω by use of Equation (5)],

$$d(\omega) = 2\sqrt{[B_e - \alpha_e(v + 1)]^2 - \alpha_e(\omega - \omega_v)} \tag{9}$$

for the entire band, including the returning R-branch.

The energy term $E_v(J)$ [Equation (6), Stull and Plass[1]] in terms of the transition frequency ω, is given by

$$E_v(J) = \frac{B_e - (v + 1)\,\alpha_e}{\alpha_e^2} \left\{ 2\left[B_e - (v + 1)\,\alpha_e\right] \left[B_e - (v + 1)\,\alpha_e \right.\right.$$

$$\left. \mp \sqrt{\left[B_e - (v + 1)\,\alpha_e\right]^2 - \alpha_e(\omega - \omega_v)}\right]$$

$$\left. - \left(1 + \frac{\frac{1}{2}\alpha_e}{B_e - (v + 1)\,\alpha_e}\right) \alpha_e(\omega - \omega_v) \right\} . \tag{10}$$

Several approximations are used in the analysis. The factor $\bar{\omega}_v^{v'}$ defined by Equation (5)[1] is approximated by

$$\bar{\omega}_v^{v'} = \omega_v \left[1 - \exp\left(-\frac{hc\omega_v}{kT}\right)\right] . \tag{11}$$

The Herman and Wallis[11] factor $F_{v\ j}^{v'\ j'}$ is approximated by

$$F = 1 + c\left[\frac{B_e - \alpha_e(v+1) \mp \sqrt{[B_e - \alpha_e(v+1)]^2 - \alpha_e(\omega - \omega_v)}}{\alpha_e}\right] \quad (12)$$

where

$$c = \frac{-\delta B_e \theta}{\omega_e} \quad (13)$$

(θ is the ratio of the zeroth to the first order term in the expansion of the electric dipole moment). The partition functions $G_R(T)$ and $G(T)$ are approximated by

$$G_R(T) = \frac{kT}{B_e hc} \quad (14)$$

and

$$G(T) = \frac{kT}{B_e hc} \frac{\exp\left[-E(0,0)\ hc/kT\right]}{1 - \exp\left(-hc\omega_v/kT\right)} . \quad (15)$$

Stull and Plass[1] give the following equation for the integrated absorption of a vibration-rotation line:

$$S_{v\ j}^{v'\ j'} = \frac{\alpha_v^{v'}\ \omega_{v\ j}^{v'\ j'}}{G_R(v,T)\ \bar{\omega}_v^{v'}} \exp\left[-E_v(j)\ \frac{hc}{kT}\right] F_{v\ j}^{v'\ j'} \times$$

$$\left[j\ \delta_{j-1,j'} + (j+1)\ \delta_{j+1,j'}\right]\left[1 - \exp\left(-\omega_{v\ j}^{v'\ j'}\ \frac{hc}{kT}\right)\right] . \quad (16)$$

Since

$$j\ \delta_{j-1,j'} + (j+1)\ \delta_{j+1,j'} = |m| ,$$

and by use of the preceding approximations, this becomes

$$S_v^{v+1(\mp)}(\omega) = \frac{\alpha_v^{v+1} B_e hc}{\bar{\omega}_v^{v+1} kT}\,\omega \left| \frac{B_e - \alpha_e(v+1) \mp \sqrt{[B_e - \alpha_e(v+1)]^2 - \alpha_e(\omega-\omega_v)}}{\alpha_e} \right| \times$$

$$\exp\left[\frac{-1.439\,[B_e - \alpha_e(v+1)]}{\alpha_e^2\, T}\left\{2[B_e - \alpha_e(v+1)]\,[B_e - \alpha_e(v+1)\right.\right.$$

$$\left.\left. \mp\sqrt{[B_e - \alpha_e(v+1)]^2 - \alpha_e(\omega-\omega_v)}\,] - \left(1 + \frac{\tfrac{1}{2}\alpha_e}{B_e - \alpha_e(v+1)}\right)\alpha_e(\omega-\omega_v)\right\}\right] \times$$

$$\left(1 + \frac{c}{\alpha_e}\left[B_e - \alpha_e(v+1) \mp \sqrt{[B_e - \alpha_e(v+1)]^2 - \alpha_e(\omega-\omega_v)}\right]\right)\left(1 - e^{\frac{-\omega hc}{kT}}\right). \tag{17}$$

Experimental data are used, where available, for the total band absorption α_v^{v+1}. A convenient approximation is made to Stull and Plass'[1] Equation (8); namely,

$$\frac{\alpha_v^{v+1}(T)}{\alpha_v^{v+1}(T_o)} = \frac{T_o}{T}\,\frac{\bar{\omega}_o^1(T)\,\bar{\omega}_v^{v+1}(T)}{\bar{\omega}_o^1(T_o)\,\bar{\omega}_v^{v+1}(T_o)} \exp\left[\left|E(v) - E(0,0)\right|\frac{hc}{k}\left(\frac{1}{T_o} - \frac{1}{T}\right)\right], \tag{18}$$

so that α_v^{v+1} can be computed for any temperature if it is known for one temperature.

If data are not available for higher-order bands, by assuming the harmonic oscillator approximation and using Stull and Plass'[1] Equations (4) and (9), one obtains

$$\frac{\alpha_v^{v'+1}(T)}{\alpha_v^{v+1}(T)} = \frac{v'+1}{v+1} \exp\left[-\left(E(v') - E(v)\right)\frac{hc}{kT}\right]. \tag{19}$$

In the weak line approximation, the emissivity is given by

$$\epsilon_\omega = 1 - \exp\left[-p\bar{S}(\omega)/d(\omega)\right] \tag{20}$$

where

$$\bar{S}(\omega) = \sum_v \left[S_v^{v+1(-)}(\omega) + S_v^{v+1(+)}(\omega)\right]. \tag{21}$$

(The sum over v includes all higher-order bands which contribute significantly to the emission in the region of the fundamental, including bands associated with isotopic species.)

An additional approximation is made in the strong line approximation:

$$\Pi_i \left[1 - \text{erf}\ (X_i)\right] \approx \exp\left(-2\pi^{-\frac{1}{2}} \Sigma_i X_i\right).$$

In general, this approximation causes a change in the emissivity of less than 5%. (It gives the same result as for the statistical model.)

In the strong line approximation,

$$\epsilon_\omega = 1 - \exp\left[-2\alpha_o^{\frac{1}{2}} (p^2 \ell)^{\frac{1}{2}} \overline{S^{\frac{1}{2}}}\ (\omega)/d(\omega)\right] \qquad (22)$$

where

$$\overline{S^{\frac{1}{2}}}\ (\omega) = \sum_v \left[\left(S_v^{v+1(-)}\ (\omega)\right)^{\frac{1}{2}} + \left(S_v^{v+1(+)}\ (\omega)\right)^{\frac{1}{2}}\right], \qquad (23)$$

and α_o is the average half-width of the line at 1-atm pressure.

A detailed discussion of the range of validity of the various approximations is given by Plass.[2] For example, Plass'[2] Figure 2 indicates that for pure CO, when $\epsilon_\omega \approx 0.6$, the weak line approximation is accurate within 10% when $\beta > 3$. (This requires the pressure to be above some minimum value which is largest ($p \approx 50$ atm) when $T \approx 1200°K$.) The strong line approximation is accurate within 10% when $\beta < 1$. (For $T \approx 1200°K$ this implies a maximum $p \approx 17$ atm.) A lower limit to the validity of the strong line approximation is imposed by the presence of Doppler broadening, which has been neglected. The Doppler and Lorentz widths are comparable for $p \approx 1/2$ atm at $T \approx 1200°K$.

For pure HF, the strong line approximation may be used for pressures up to a certain value (a maximum $p \approx 35$ atm for $T \approx 3000°K$) and above a minimum determined by the Doppler broadening. (The Doppler and Lorentz widths are comparable for $p \approx 0.4$ atm and $T \approx 3000°K$.)

III. DISCUSSION

Results of this analysis are presented (Figures 1 to 32) for HCℓ, HF, CO, and NO for temperatures ranging from 300 to 7000°K. The presence of isotopes other than Cl^{35} and Cl^{37} was ignored. Emission from as many as 20 bands was considered.

Data of Benedict, et al.,[3] for HCℓ were used to make a direct comparison with the more elaborate calculations of Stull and Plass.[1] Their value of 130 ± 7 cm^{-2} atm^{-1} for the fundamental band strength is probably too low (cf. Babrov, et al.,[4] 150 ± 5 cm^{-2} atm^{-1}; Weber and Penner,[5] 150 cm^{-2} atm^{-1}).

Benedict and Plyler's[6] value of 260 cm^{-2} atm^{-1} was used for the CO fundamental band strength (cf. Weber and Penner,[5] 237 cm^{-2} atm^{-1}). Kuipers' data[7] were used for HF, and Weber and Penner's[5] for NO.

Average line widths were computed as described by Stull and Plass.[1] It should be noted that the supplementary computation made by these authors for emission from line wings in the frequency range beyond a band head is omitted here.

From 20 to 50 points were computed for each curve. Each set of four curves represents a charge of between 0.01 and 0.02 hour's time on an IBM 704 digital computer.

A comparison is made (Figures 33 and 34) with other published computations of diatomic gas emissivities. Figure 33 compares Equation (20) to the results of one particular computation by Stull and Plass[1] (for HCℓ at 2400°K in the weak line approximation for $p\ell$ = 100 atm-cm) in which they considered the emission from approximately 2900 individual spectral lines. Penner and Gray[8] recently published a comparative computation based on a simple harmonic oscillator model, which is also shown in Figure 33.

The curve representing Equation (20) follows quite closely the curve computed by Stull and Plass,[1] which is presumably the most accurate available theoretical computation. The agreement would be slightly closer

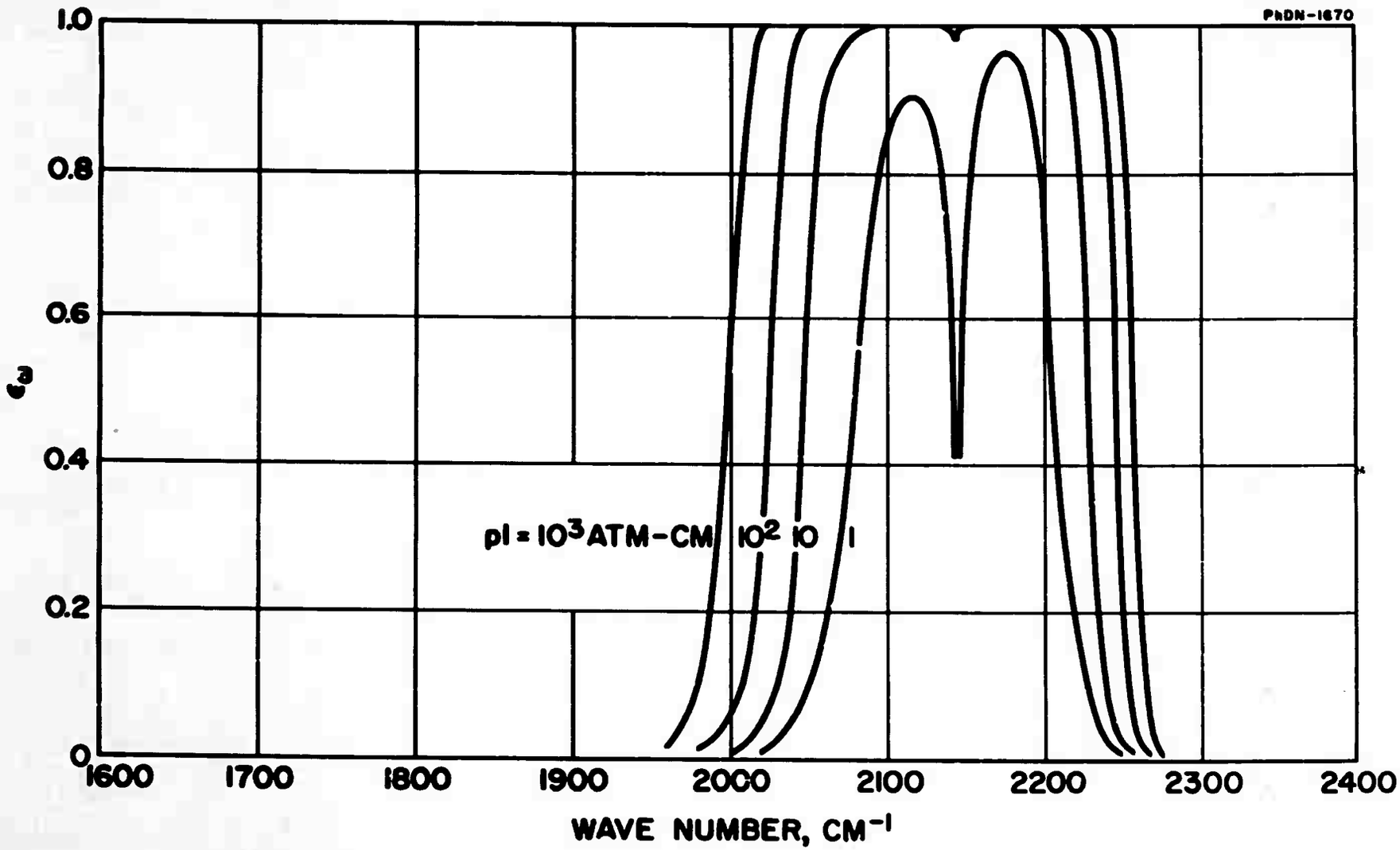

FIGURE 1 SPECTRAL EMISSIVITY OF CO AT T = 300°K
(WEAK LINE APPROXIMATION)

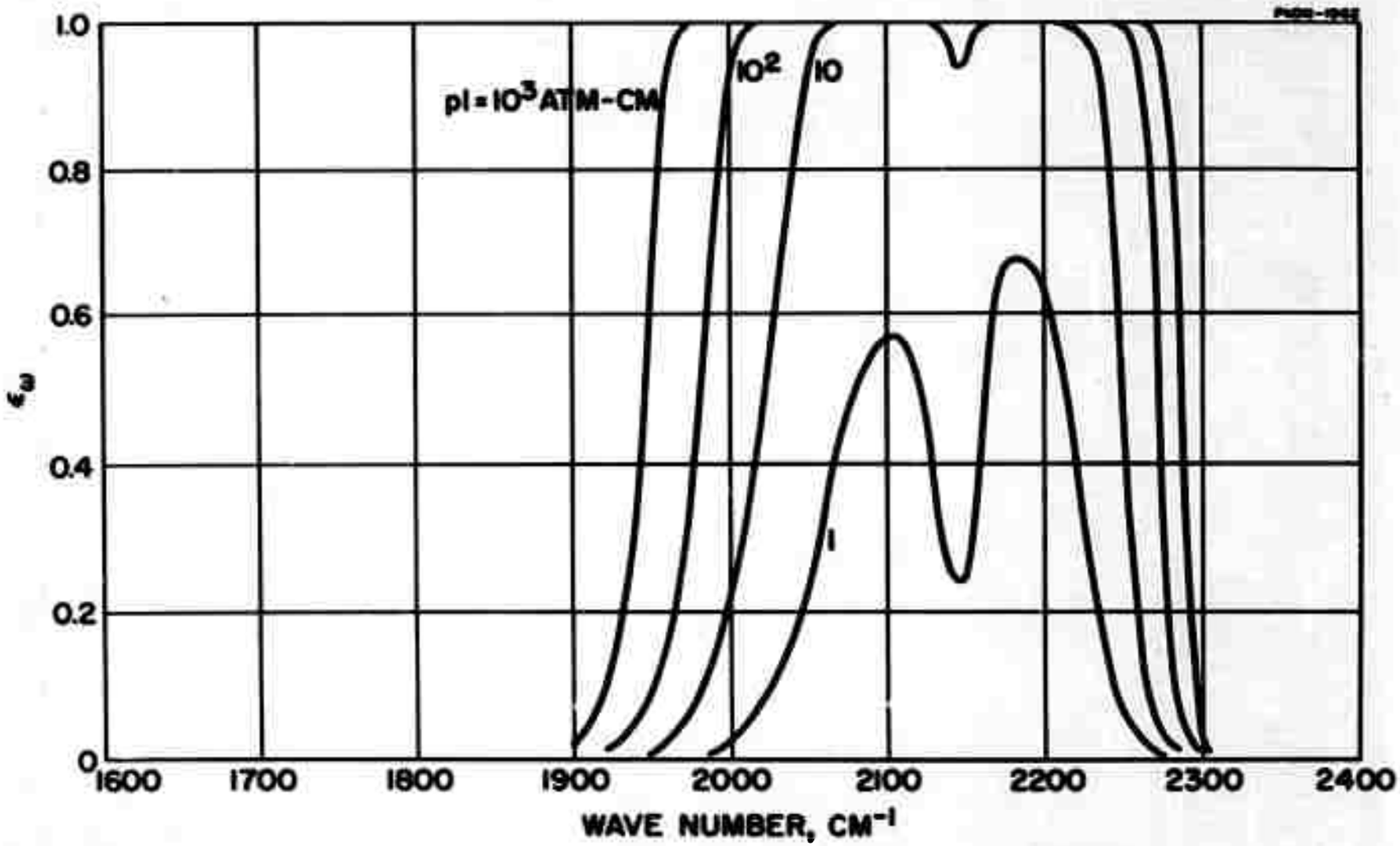

FIGURE 2 SPECTRAL EMISSIVITY OF CO AT T = 600°K
(WEAK LINE APPROXIMATION)

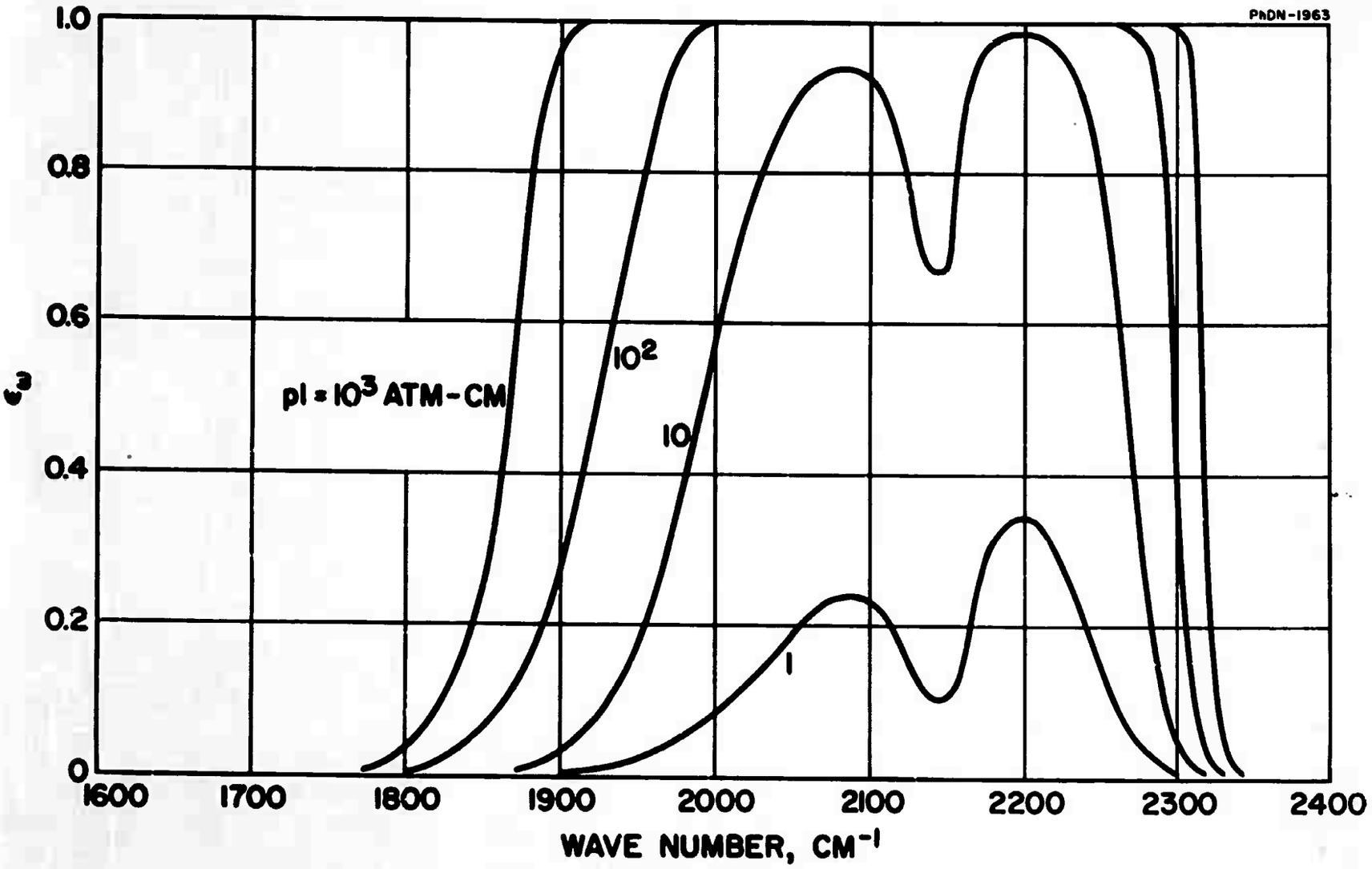

FIGURE 3 SPECTRAL EMISSIVITY OF CO AT T = 1200°K
(WEAK LINE APPROXIMATION)

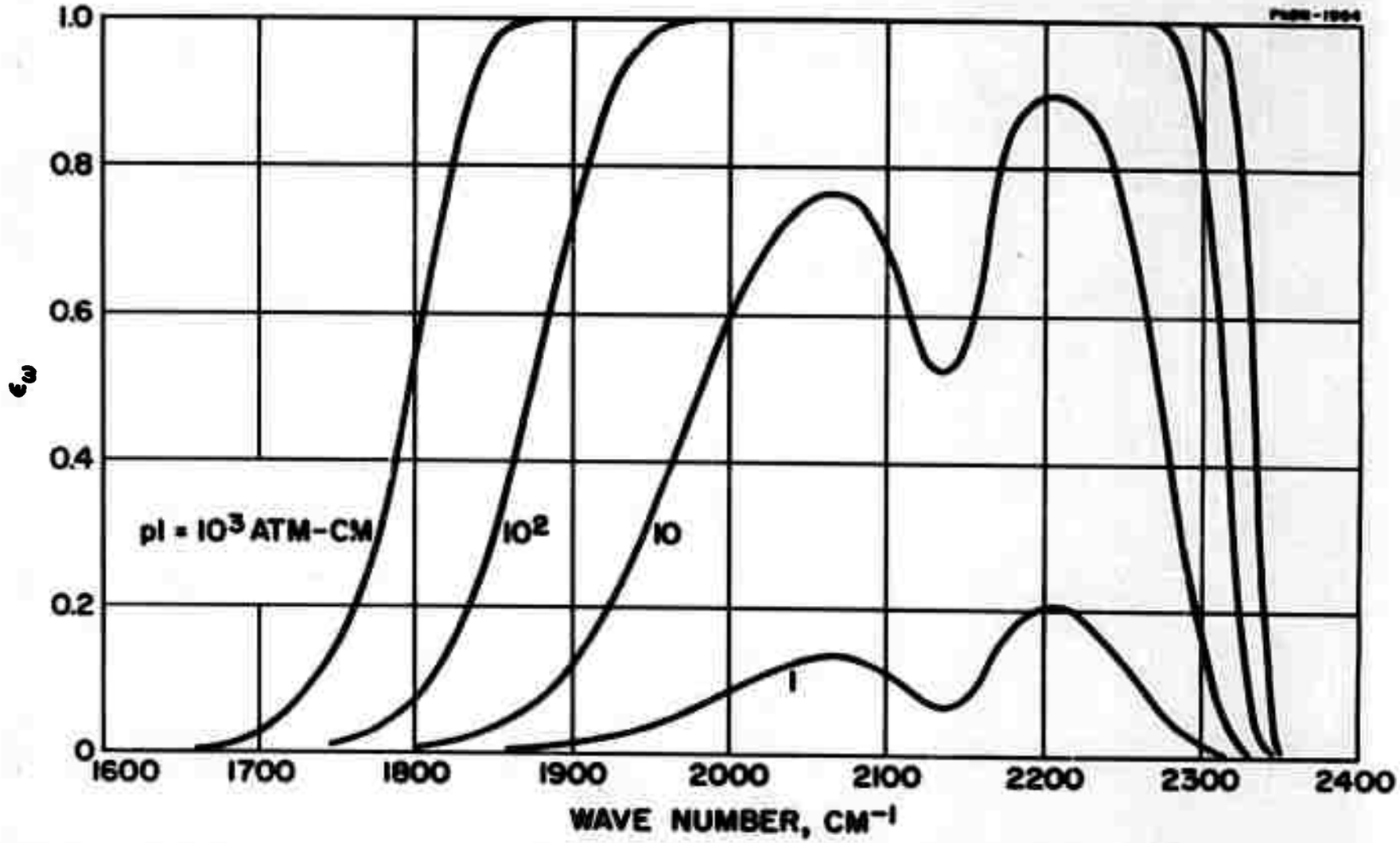

FIGURE 4 SPECTRAL EMISSIVITY OF CO AT T = 1800°K
(WEAK LINE APPROXIMATION)

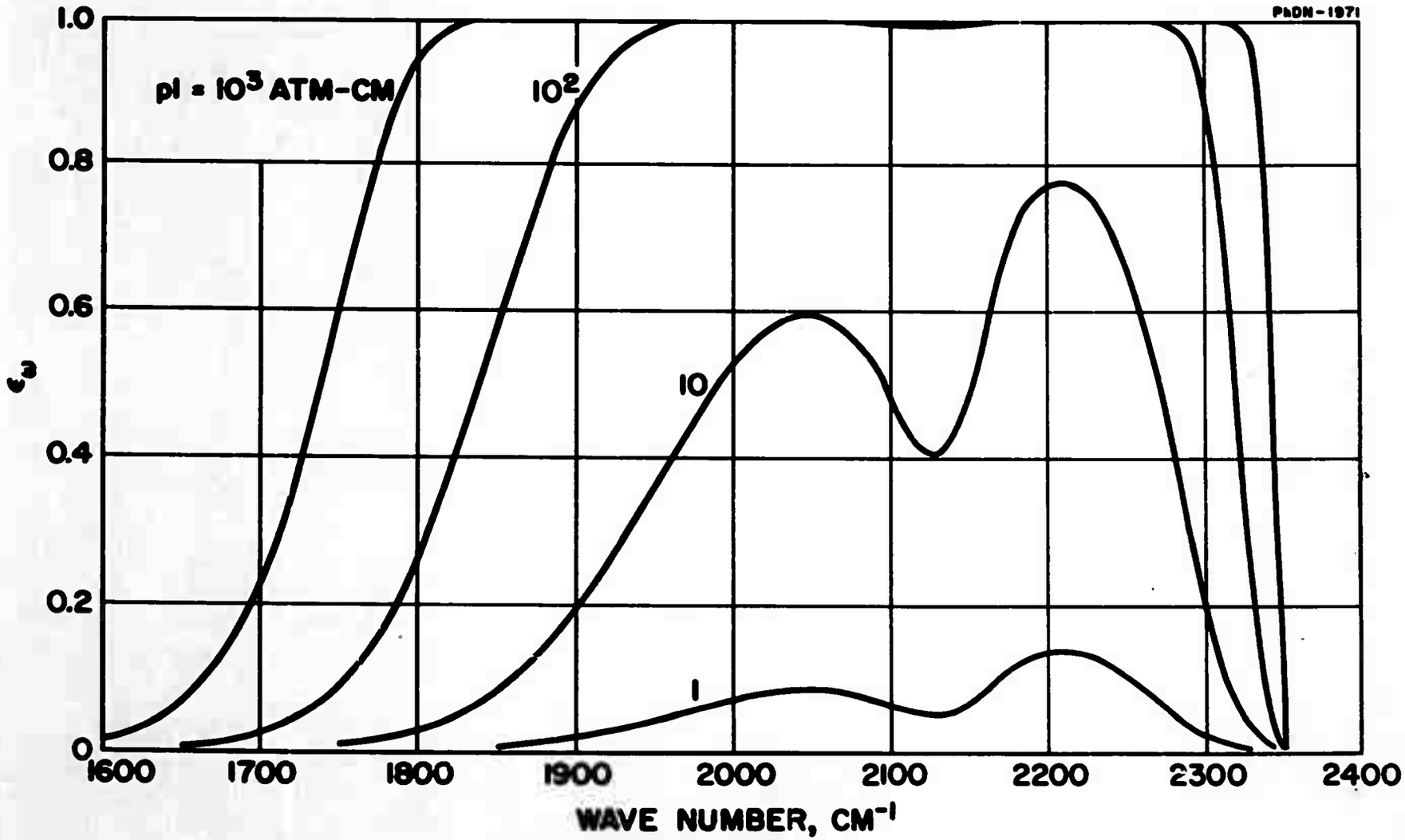

FIGURE 5 SPECTRAL EMISSIVITY OF CO AT T = 2400°K
(WEAK LINE APPROXIMATION)

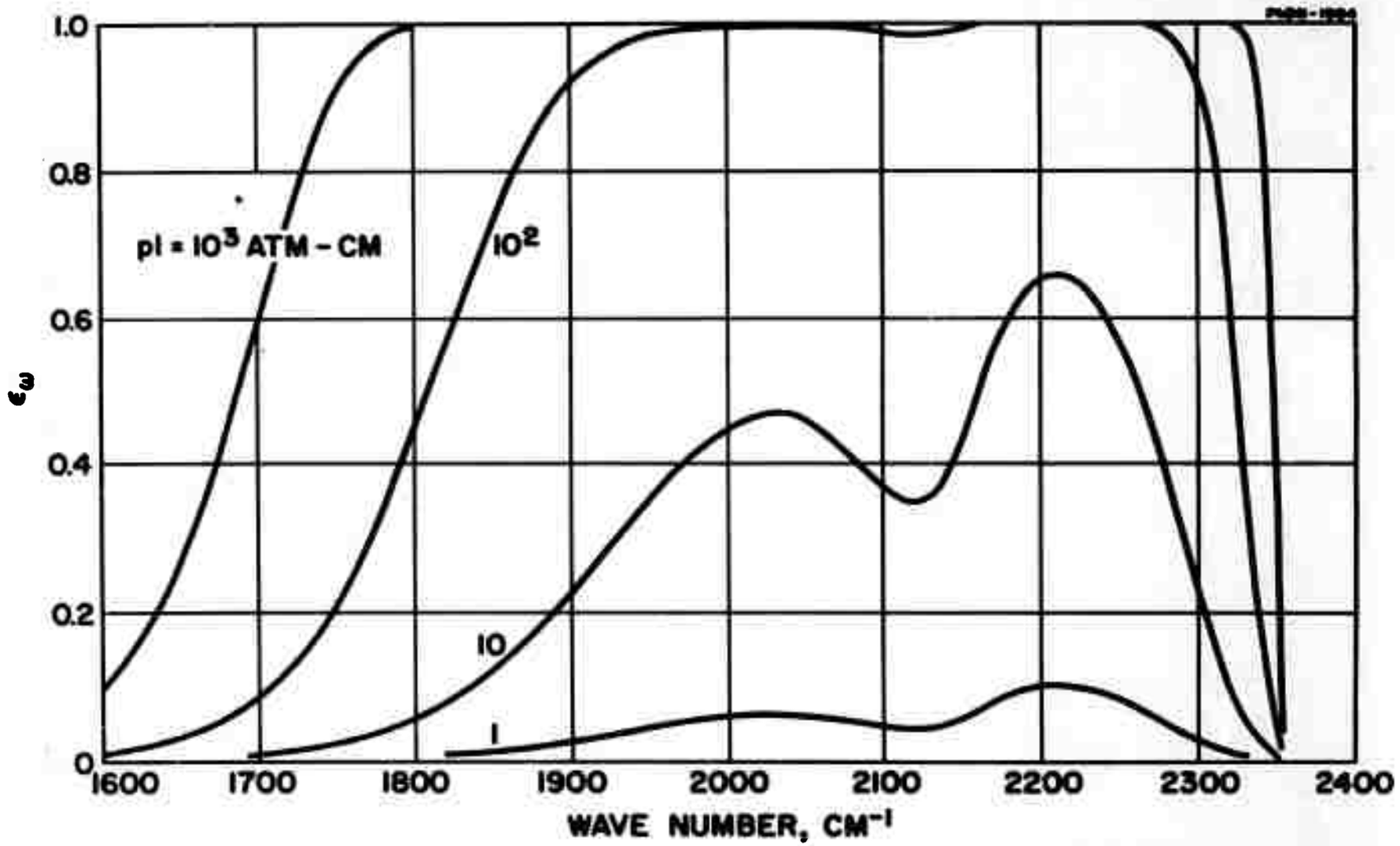

FIGURE 6 SPECTRAL EMISSIVITY OF CO AT T=3000°K
(WEAK LINE APPROXIMATION)

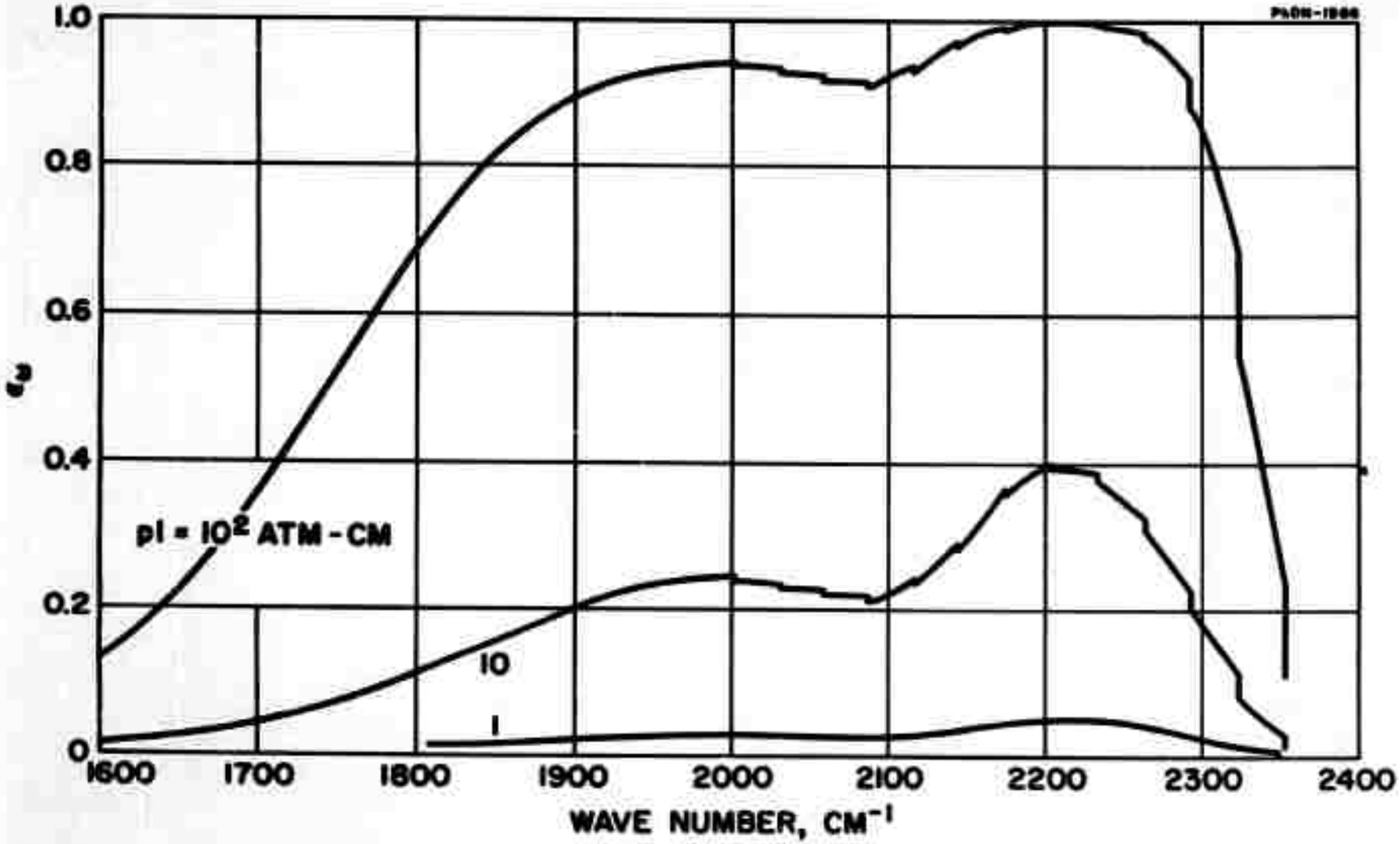

FIGURE 7 SPECTRAL EMISSIVITY OF CO AT T = 5000°K
(WEAK LINE APPROXIMATION)

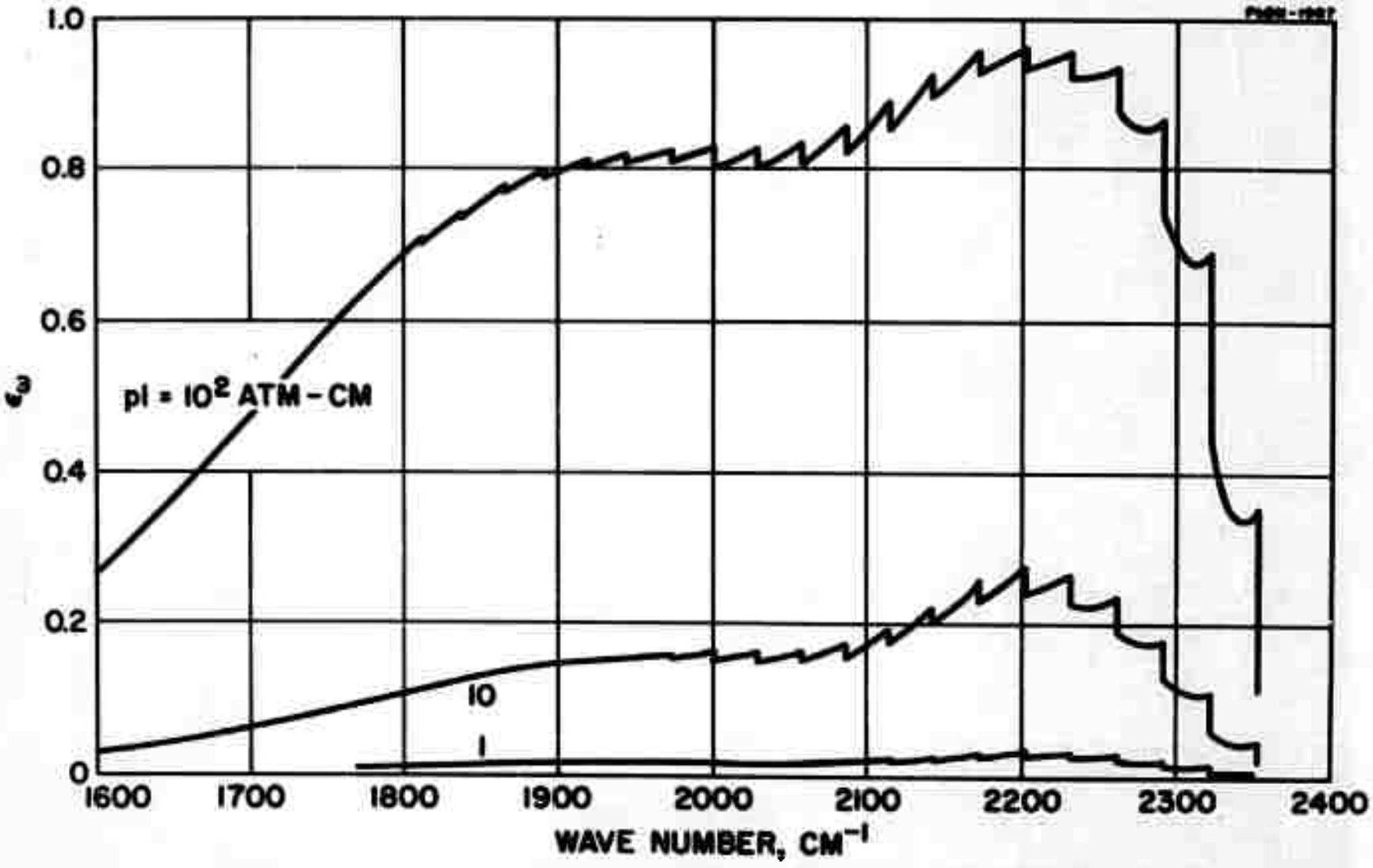

FIGURE 8 SPECTRAL EMISSIVITY OF CO AT T=7000°K
(WEAK LINE APPROXIMATION)

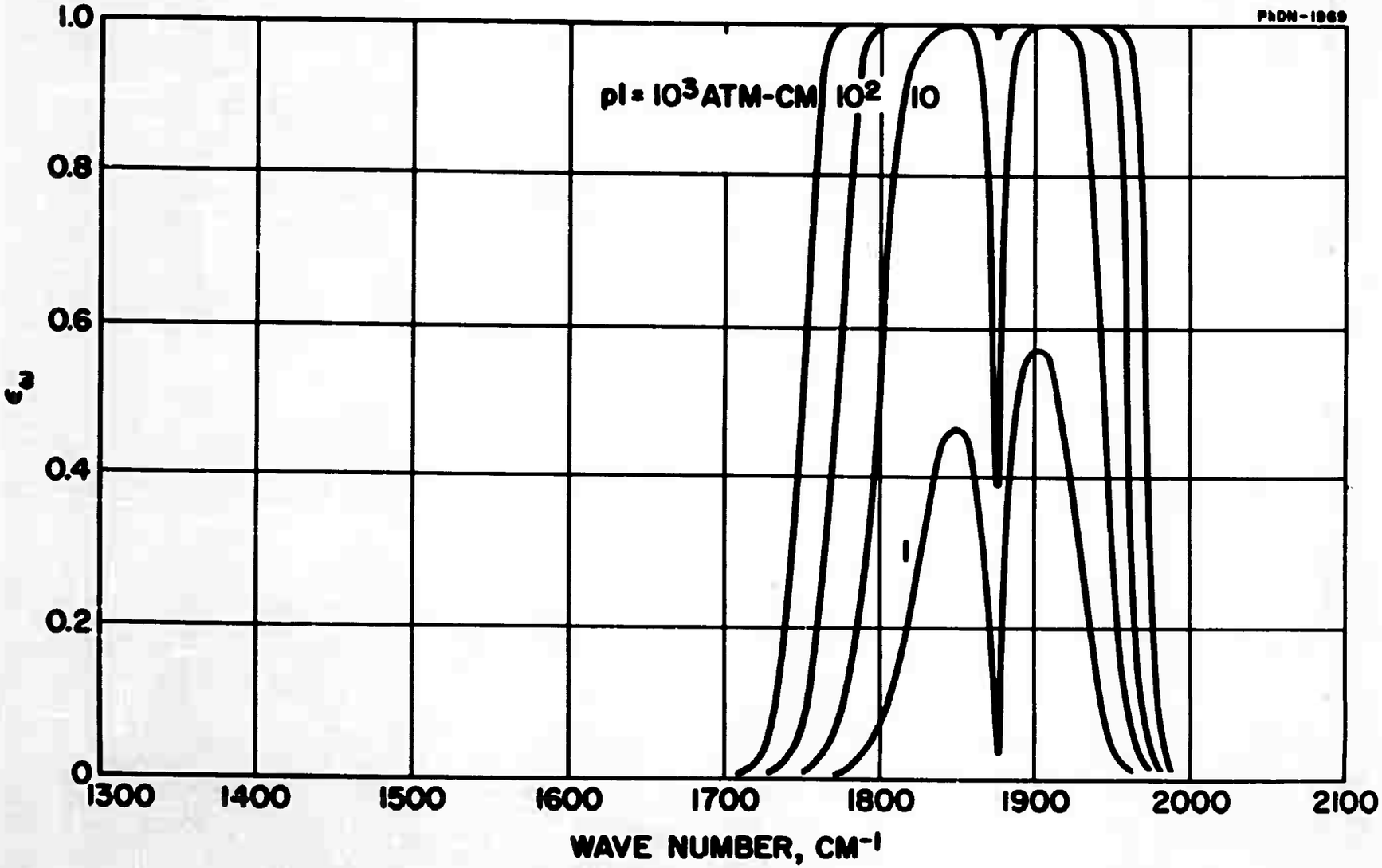

FIGURE 9 SPECTRAL EMISSIVITY OF NO AT T = 300°K
(WEAK LINE APPROXIMATION)

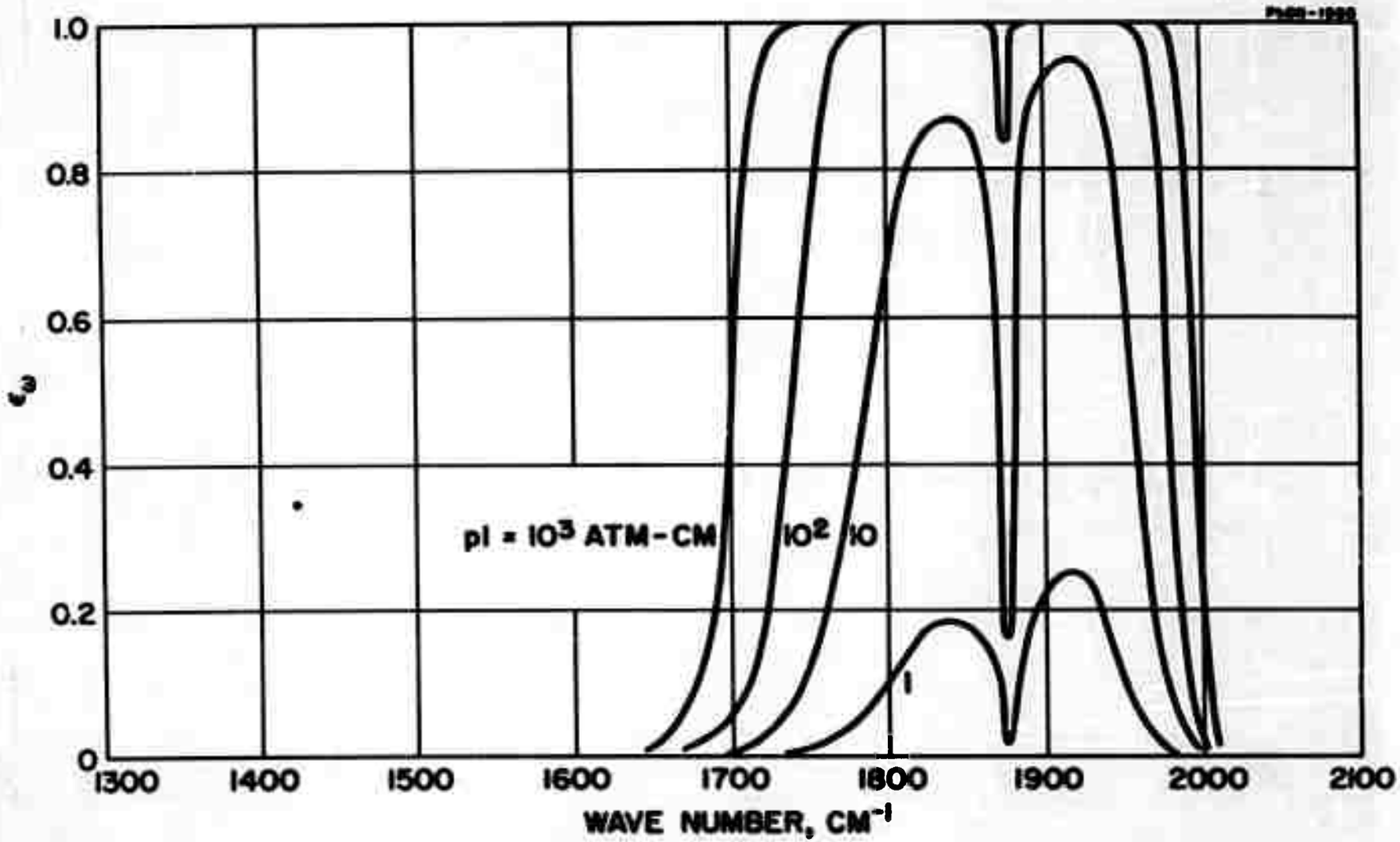

FIGURE 10 SPECTRAL EMISSIVITY OF NO AT T = 600°K
(WEAK LINE APPROXIMATION)

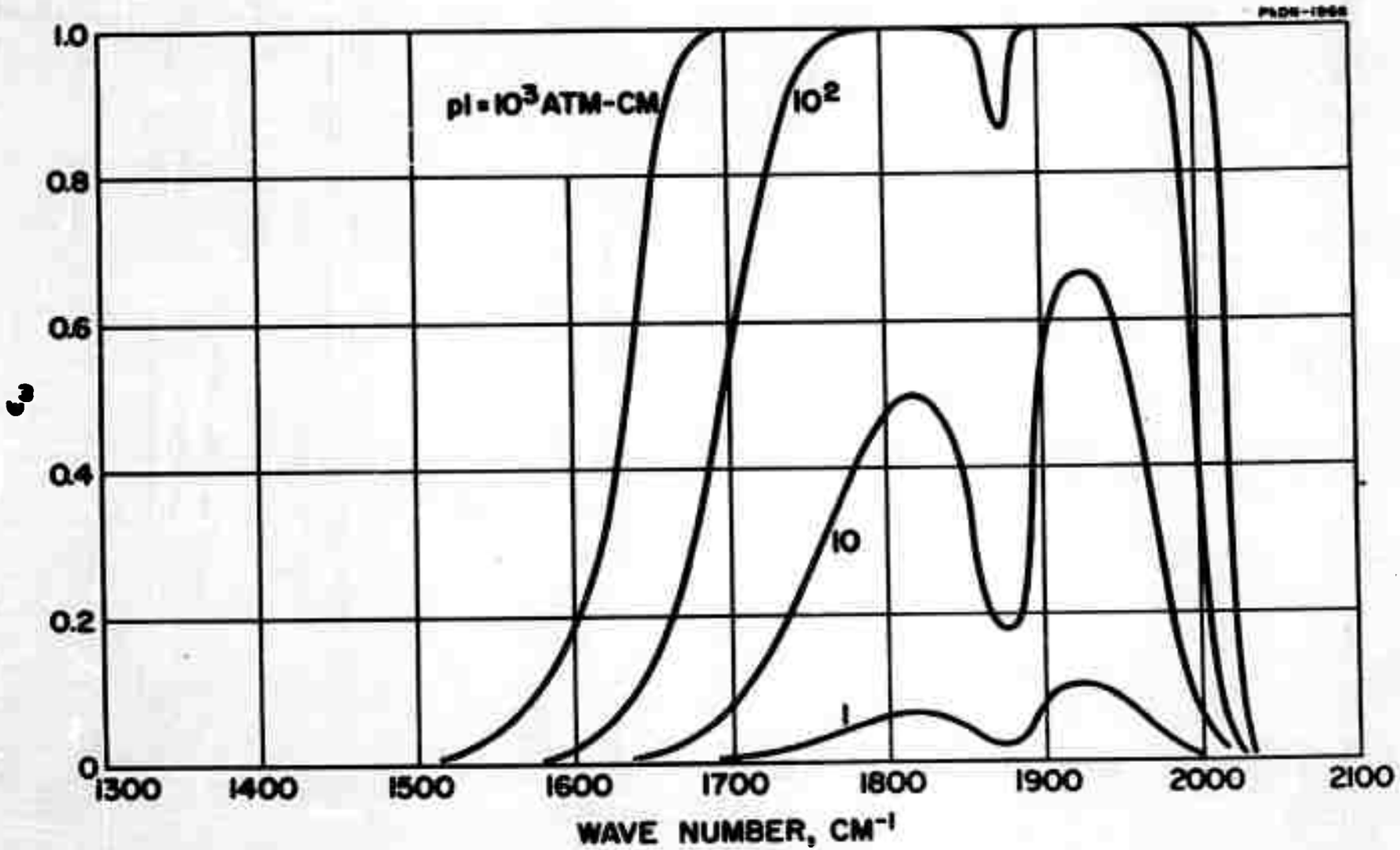

FIGURE 11 SPECTRAL EMISSIVITY OF NO AT T = 1200°K
(WEAK LINE APPROXIMATION)

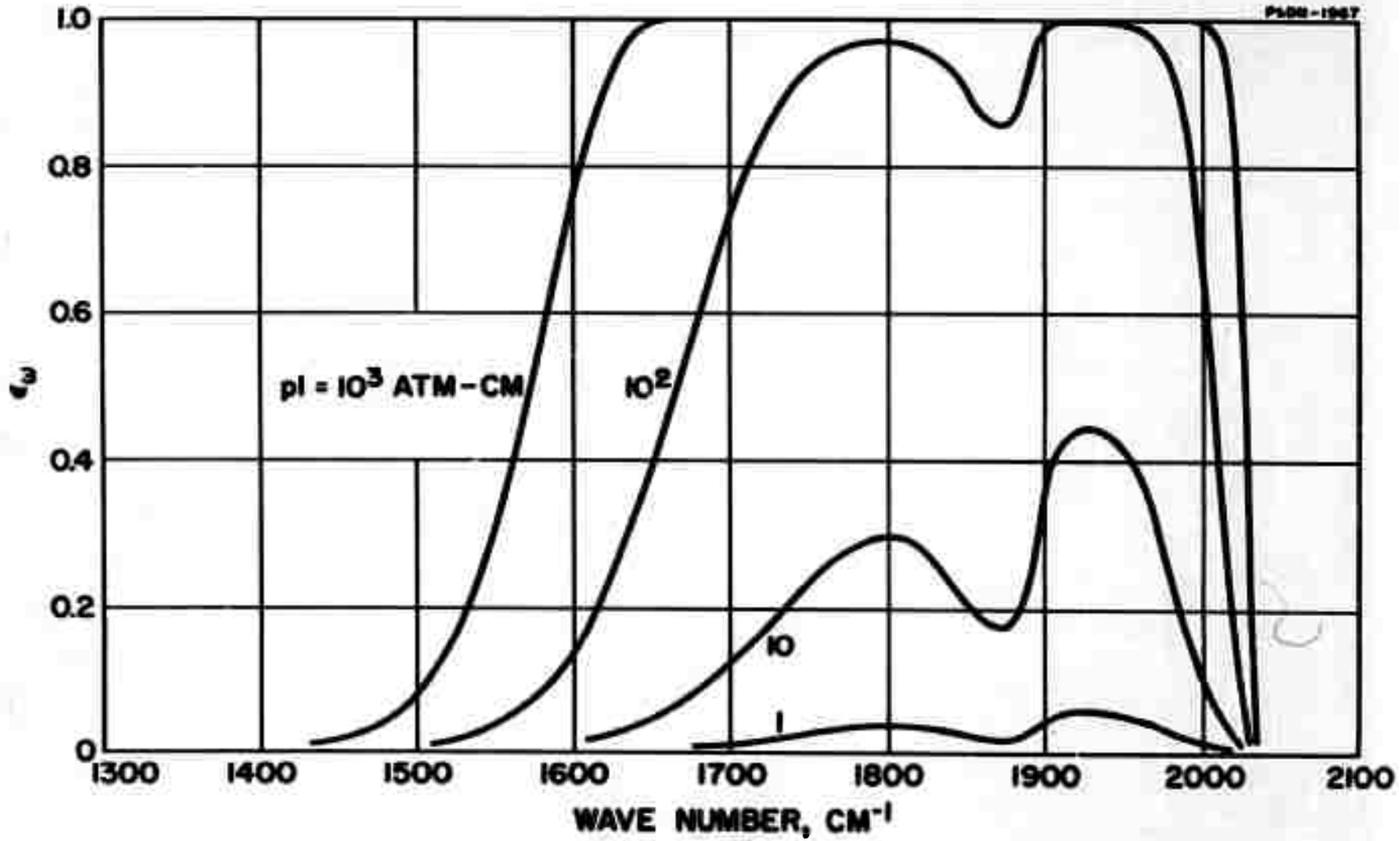

FIGURE 12 SPECTRAL EMISSIVITY OF NO AT T = 1800°K
(WEAK LINE APPROXIMATION)

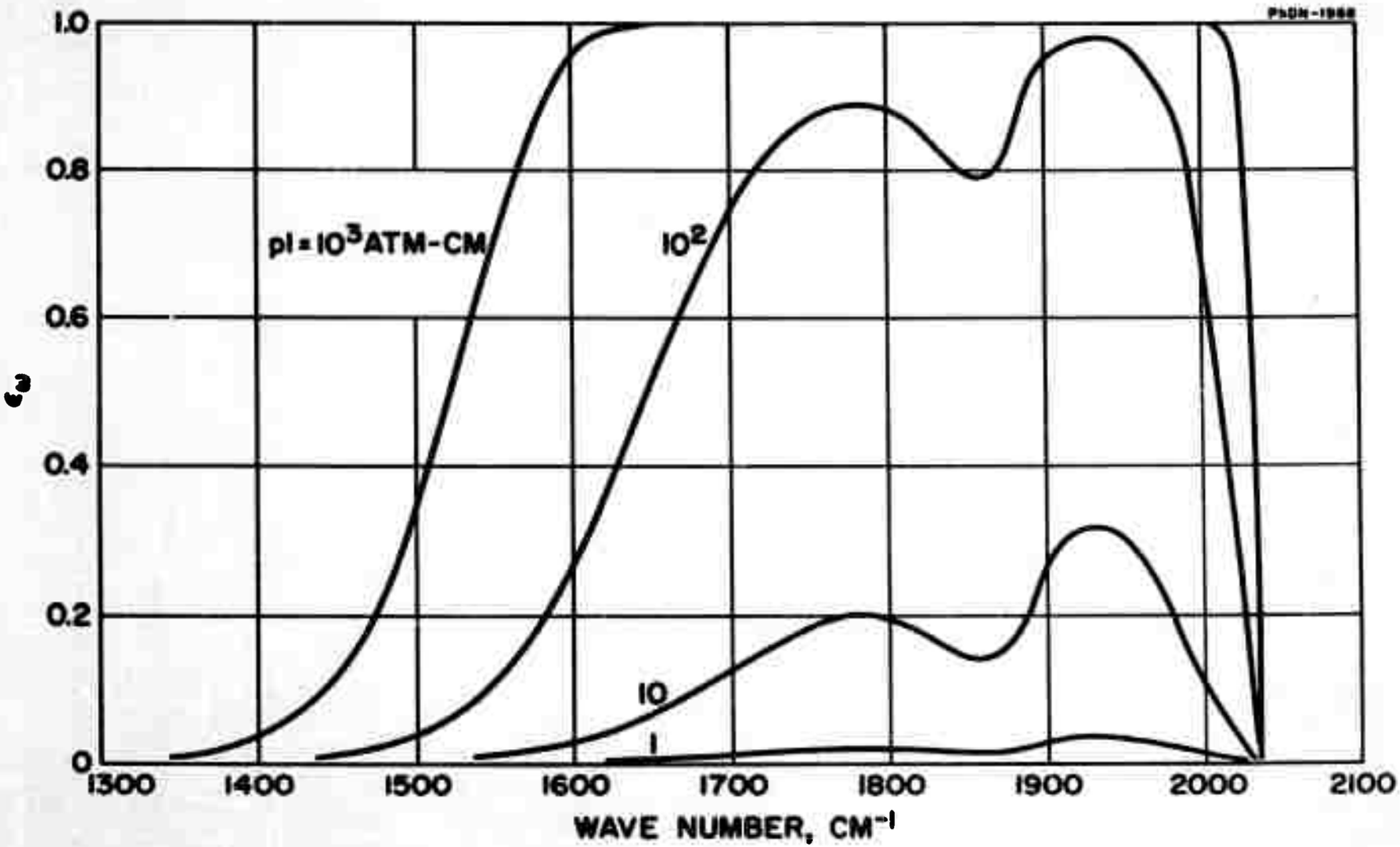

FIGURE 13 SPECTRAL EMISSIVITY OF NO AT T = 2400°K
(WEAK LINE APPROXIMATION)

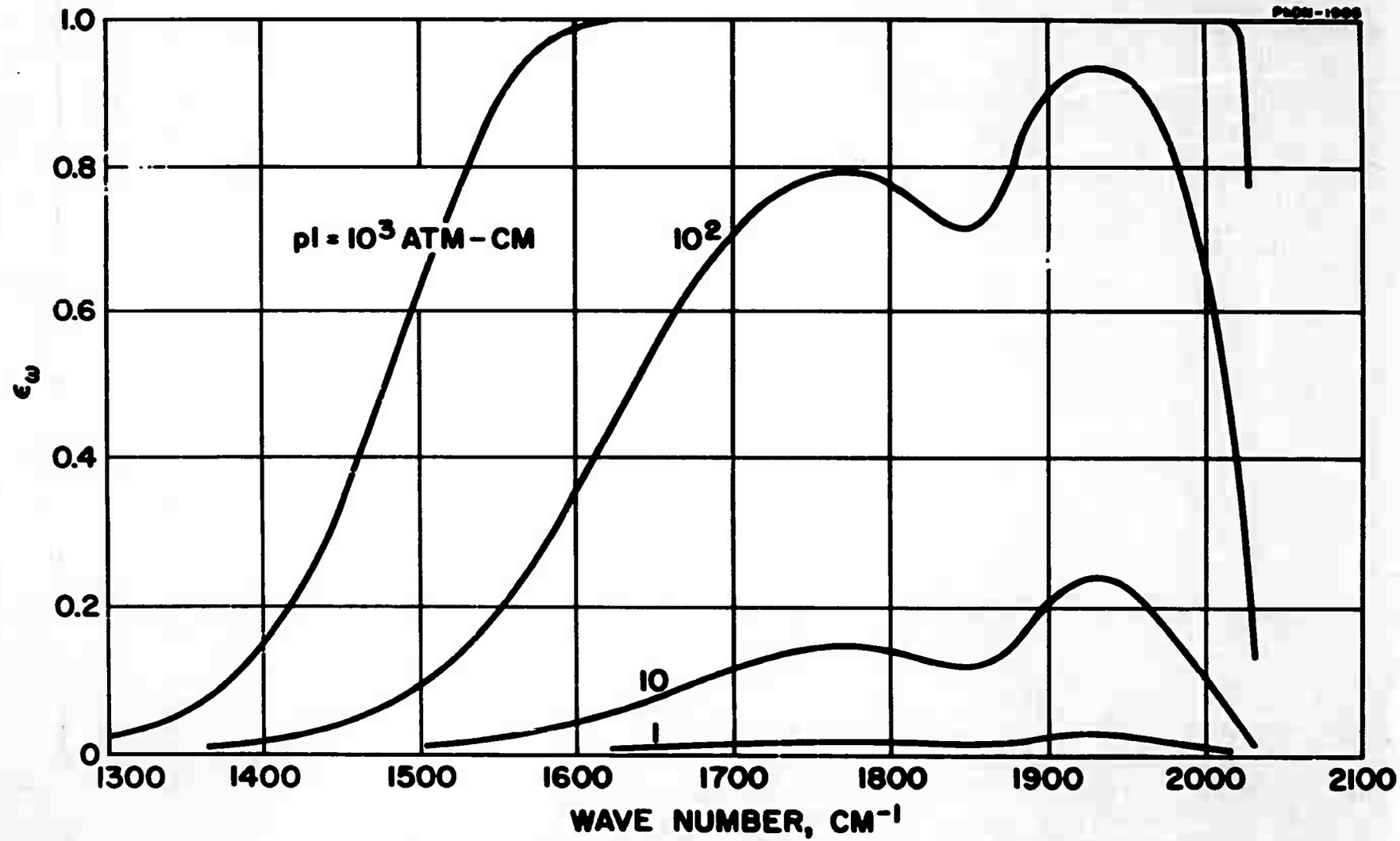

FIGURE 14 SPECTRAL EMISSIVITY OF NO AT T = 3000°K
(WEAK LINE APPROXIMATION)

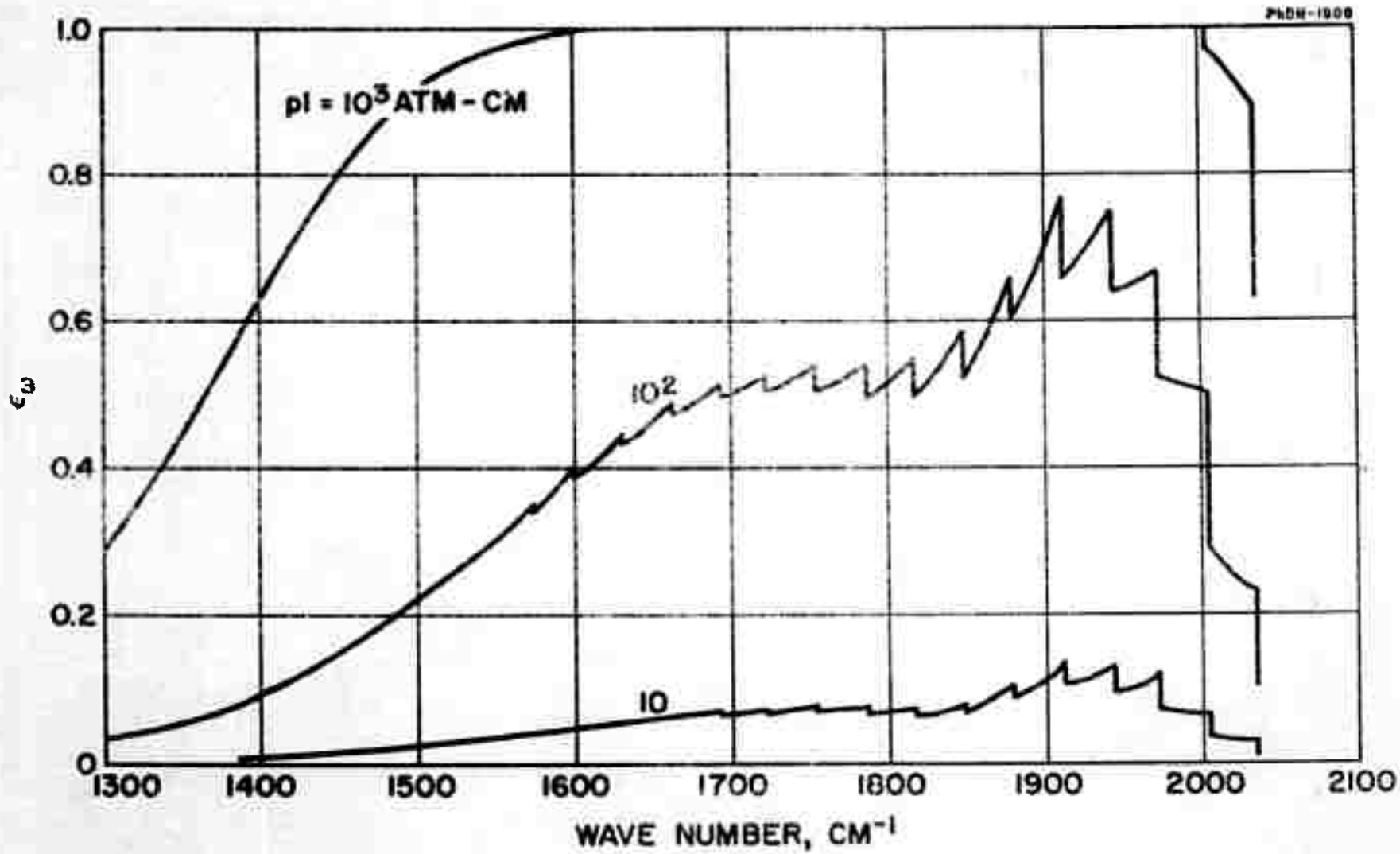

FIGURE 15 SPECTRAL EMISSIVITY OF NO AT T = 5000°K
(WEAK LINE APPROXIMATION)

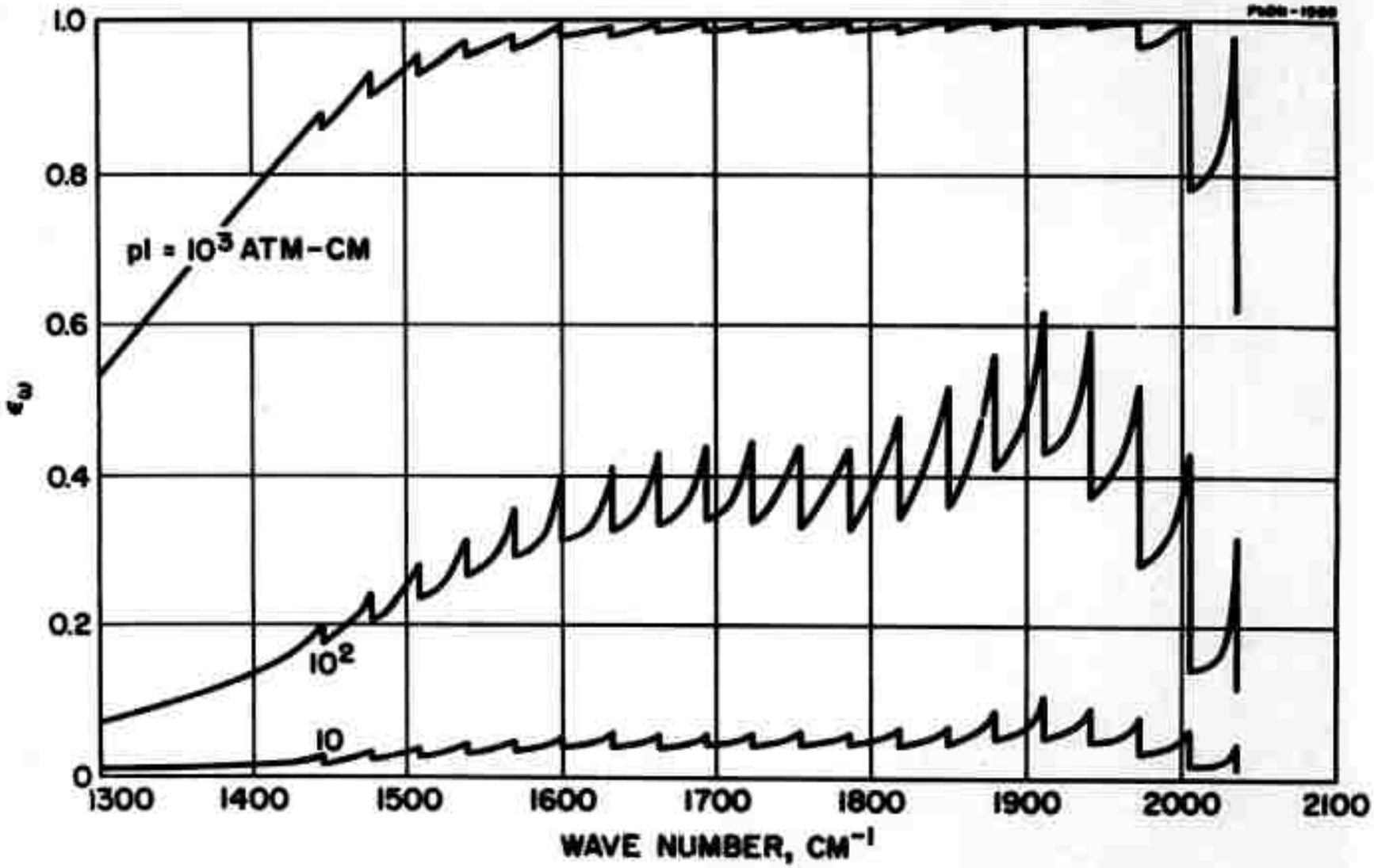

FIGURE 16 SPECTRAL EMISSIVITY OF NO AT T=7000°K
(WEAK LINE APPROXIMATION)

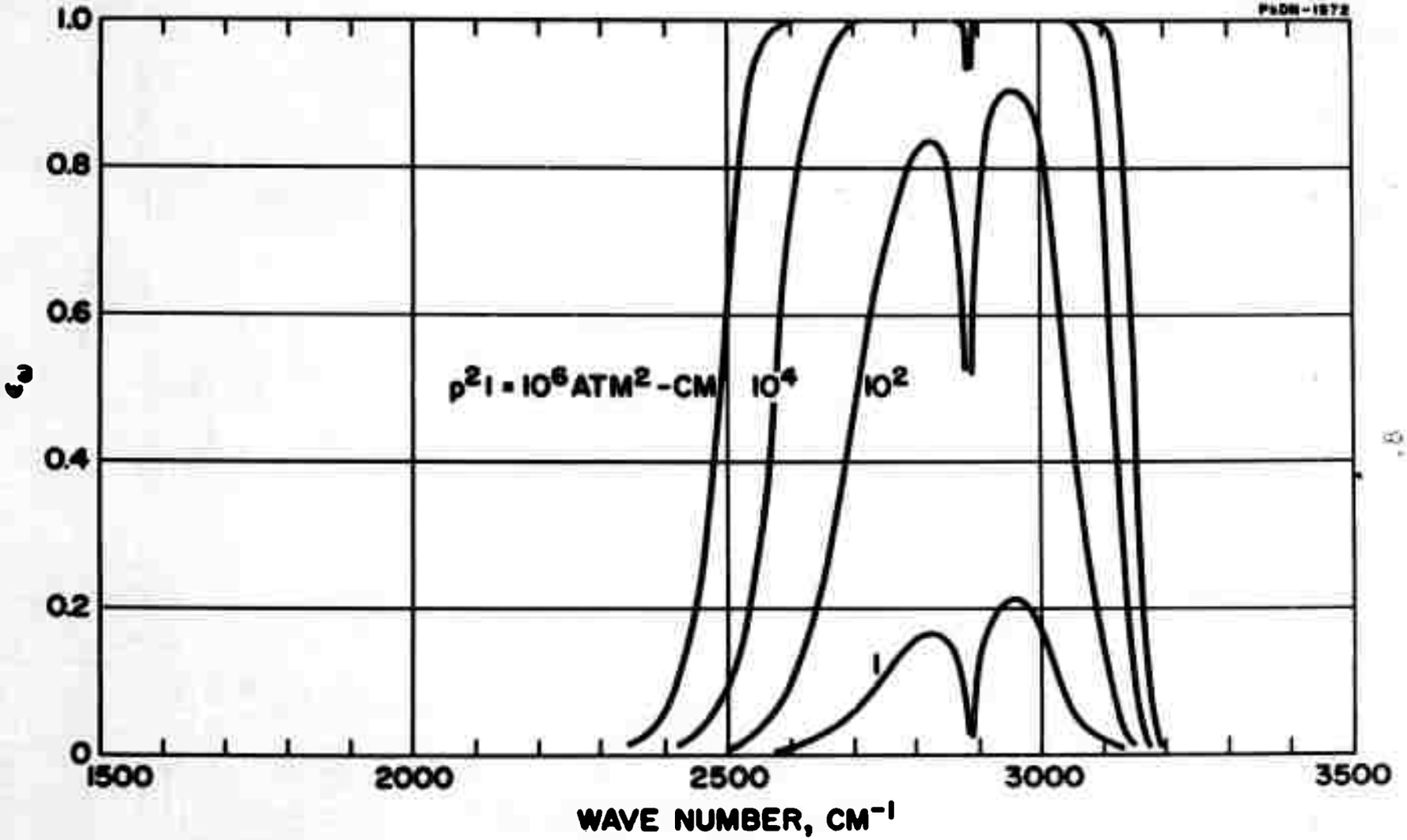

FIGURE 17 SPECTRAL EMISSIVITY OF HCℓ AT T = 300°K
(STRONG LINE APPROXIMATION)

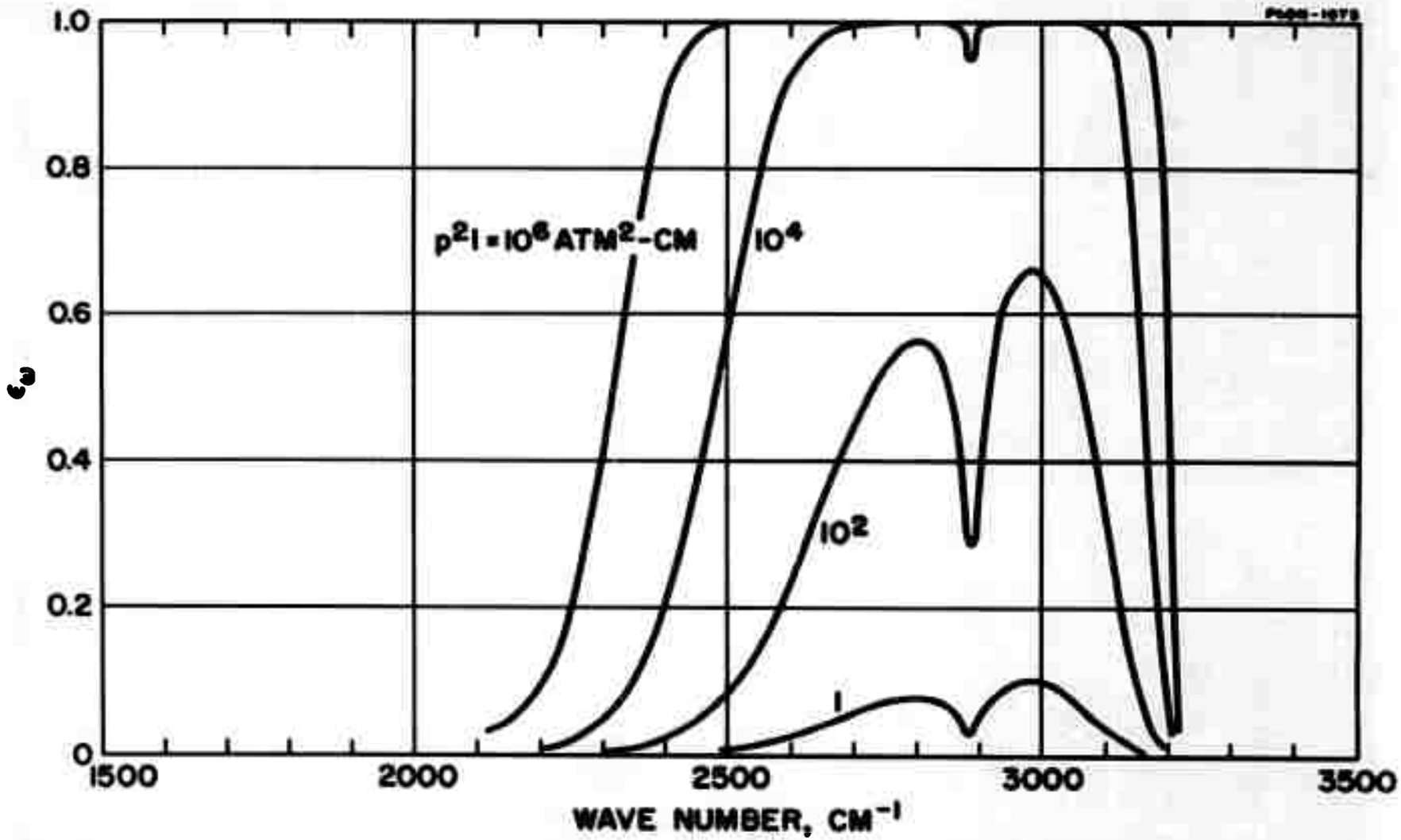

FIGURE 18 SPECTRAL EMISSIVITY OF HCℓ AT T = 600°K
(STRONG LINE APPROXIMATION)

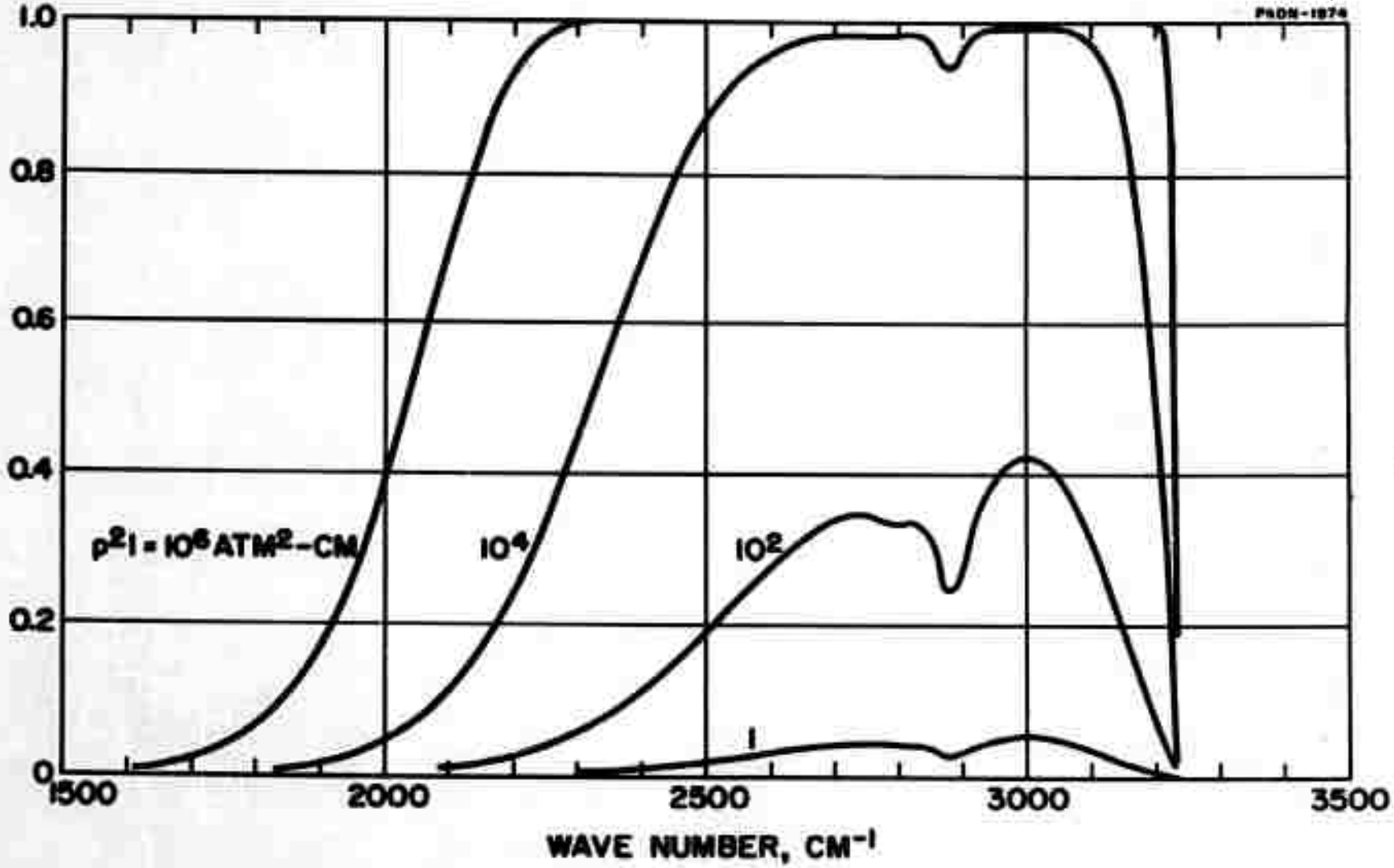

FIGURE 19 SPECTRAL EMISSIVITY OF HCℓ AT T = 1200°K
(STRONG LINE APPROXIMATION)

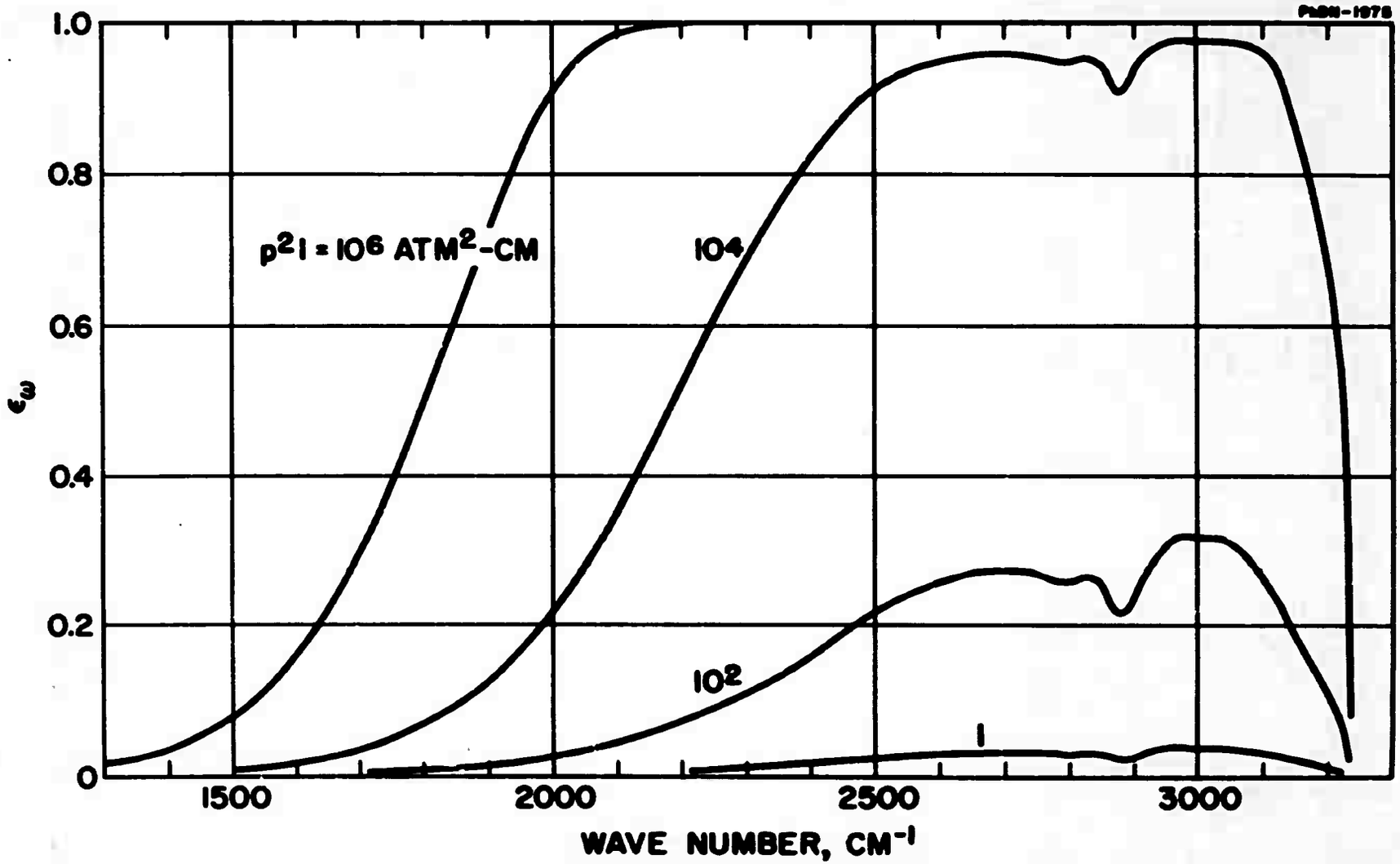

FIGURE 20 SPECTRAL EMISSIVITY OF HCℓ AT T = 1800°K
(STRONG LINE APPROXIMATION)

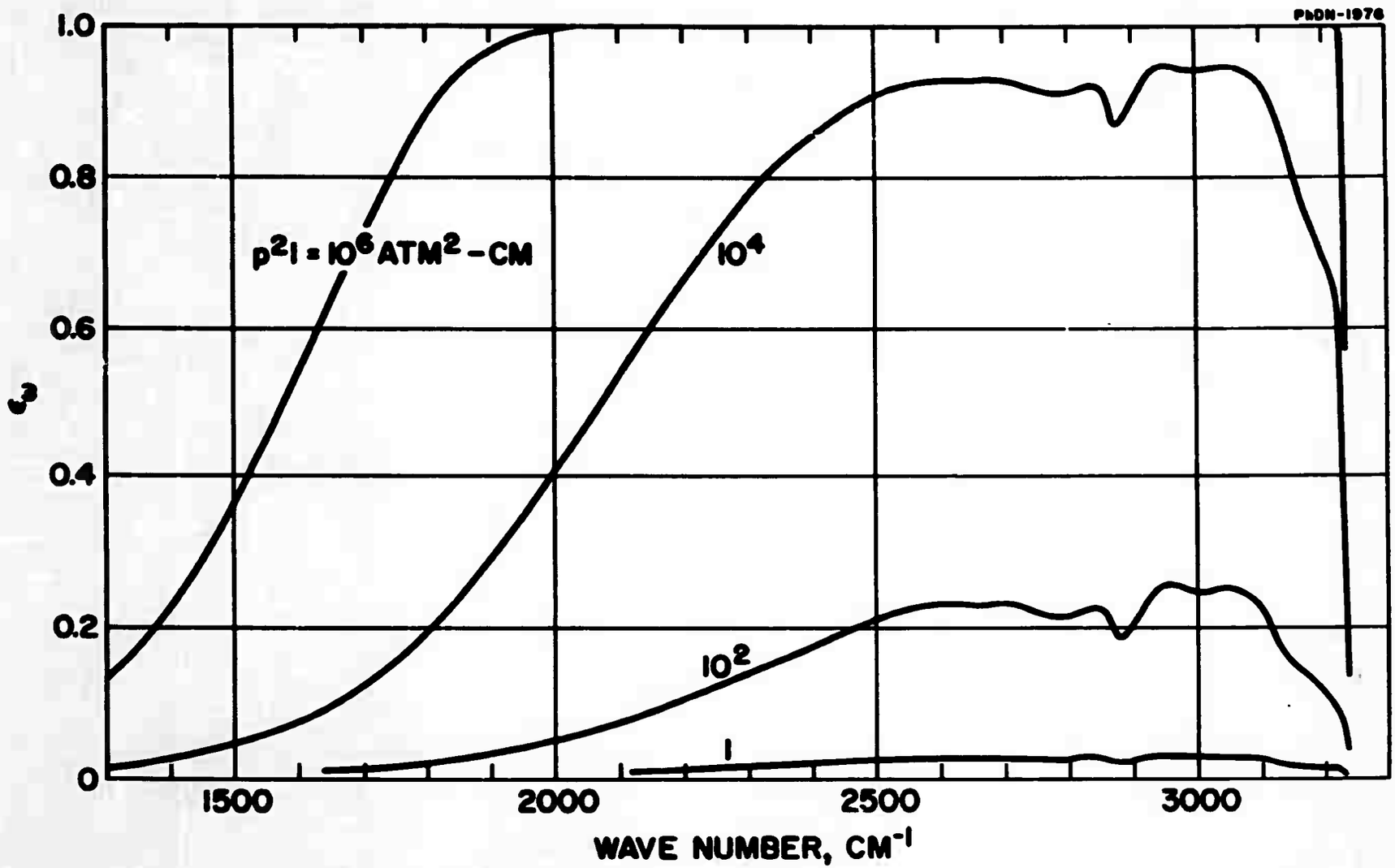

FIGURE 21 SPECTRAL EMISSIVITY OF HCℓ AT T = 2400°K
(STRONG LINE APPROXIMATION)

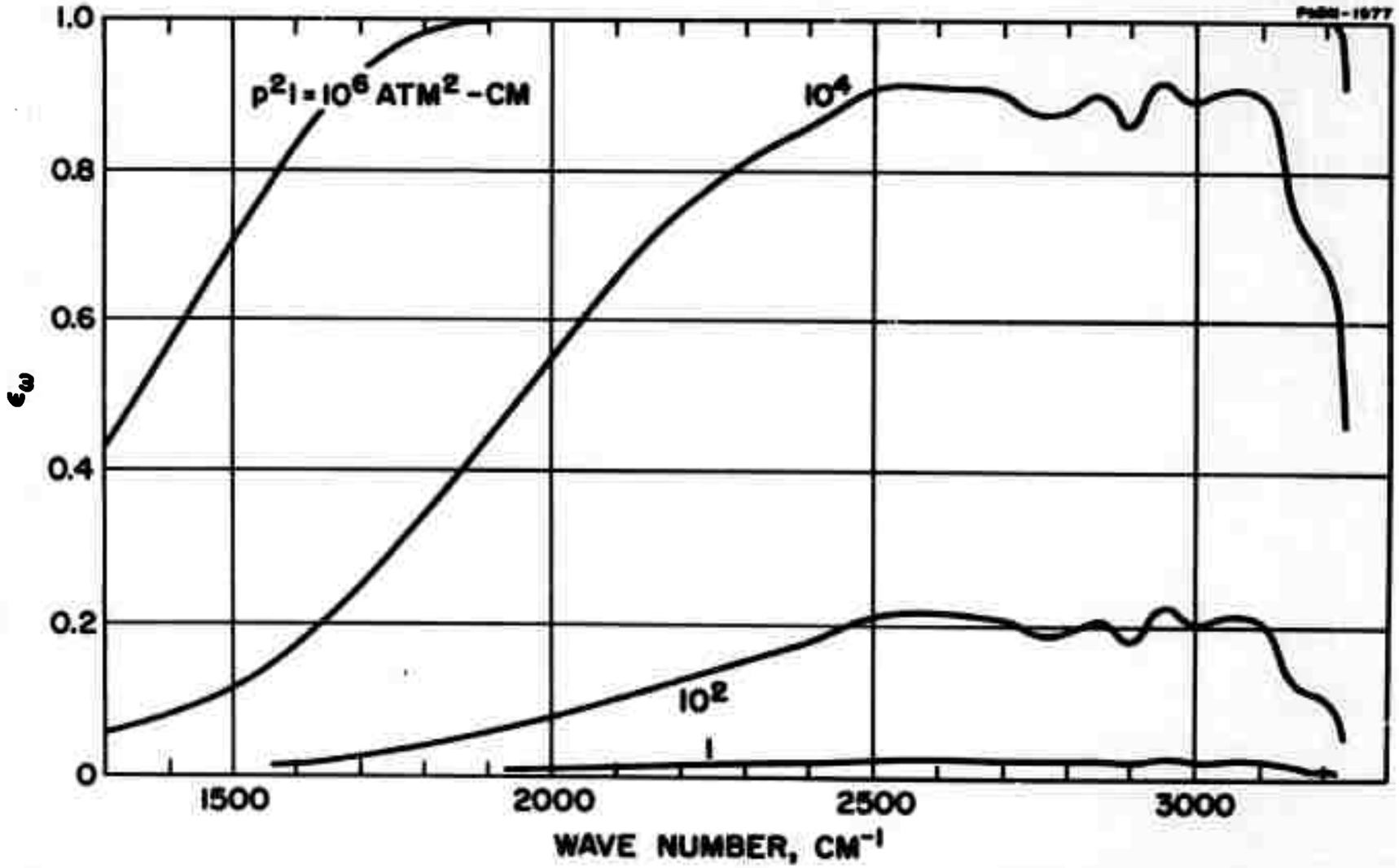

FIGURE 22 SPECTRAL EMISSIVITY OF HCℓ AT T = 3000°K (STRONG LINE APPROXIMATION)

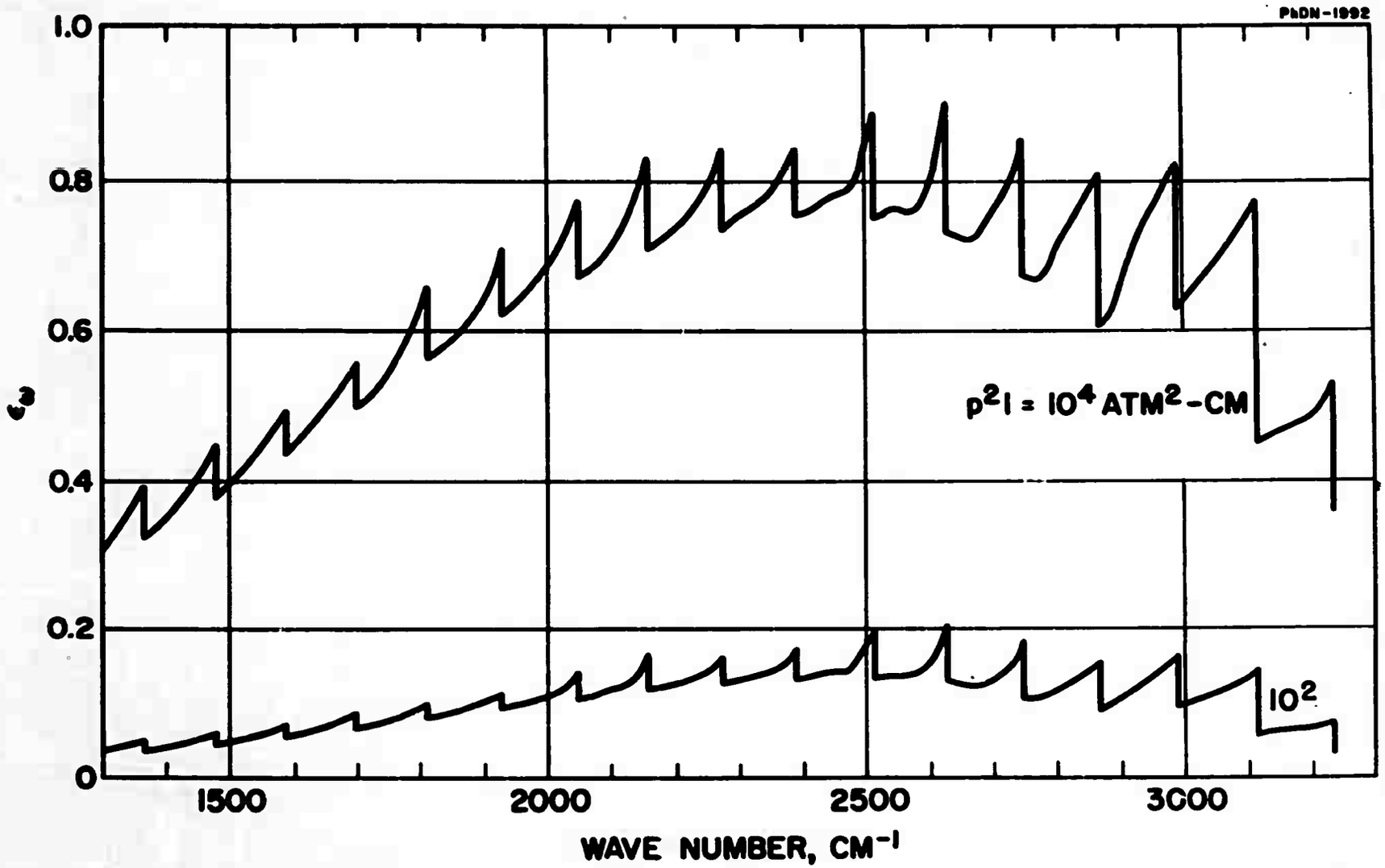

FIGURE 23 SPECTRAL EMISSIVITY OF HCℓ AT T = 5000°K
(STRONG LINE APPROXIMATION)

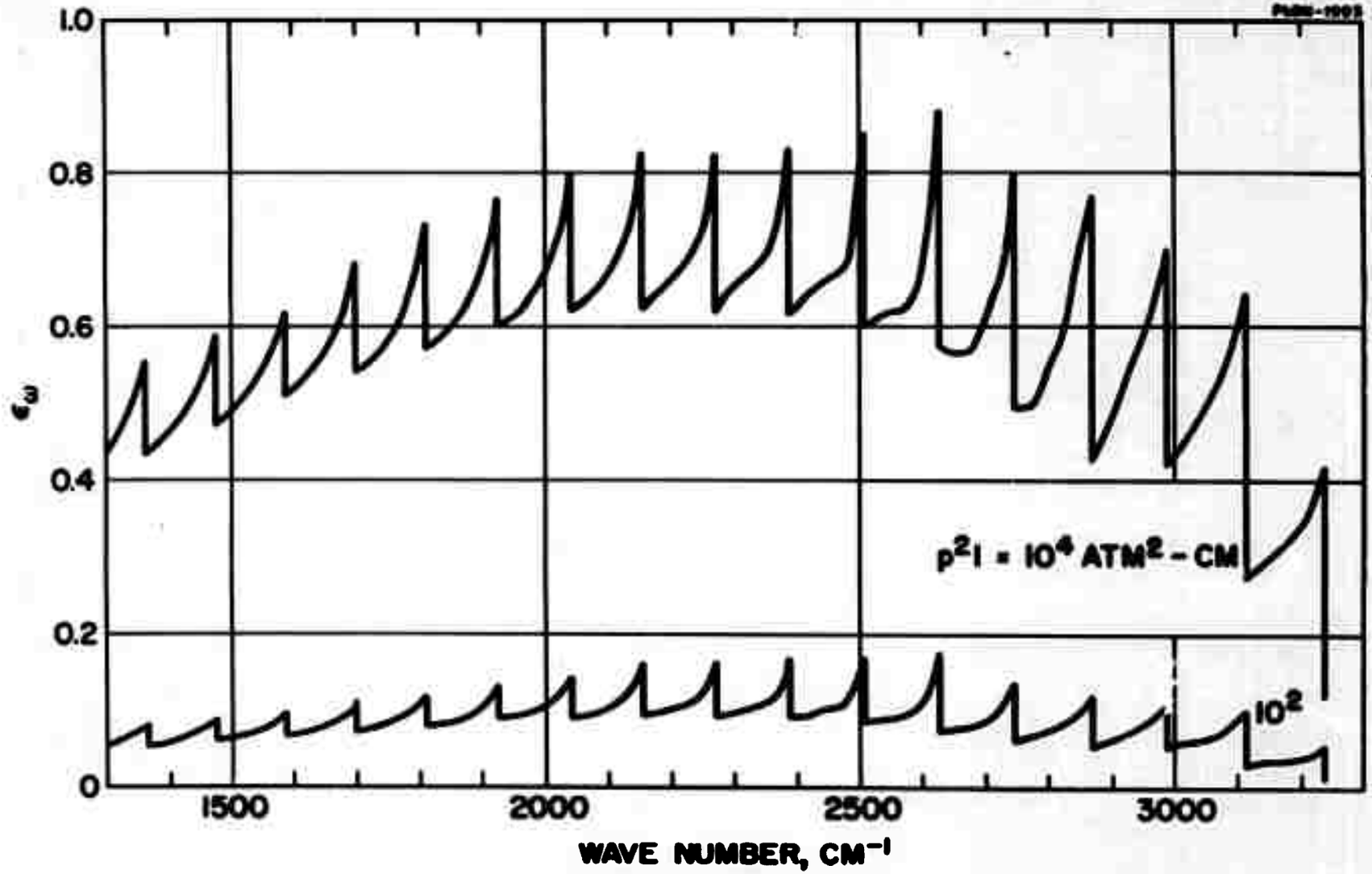

FIGURE 24 SPECTRAL EMISSIVITY OF HCl AT T=7000°K
(STRONG LINE APPROXIMATION)

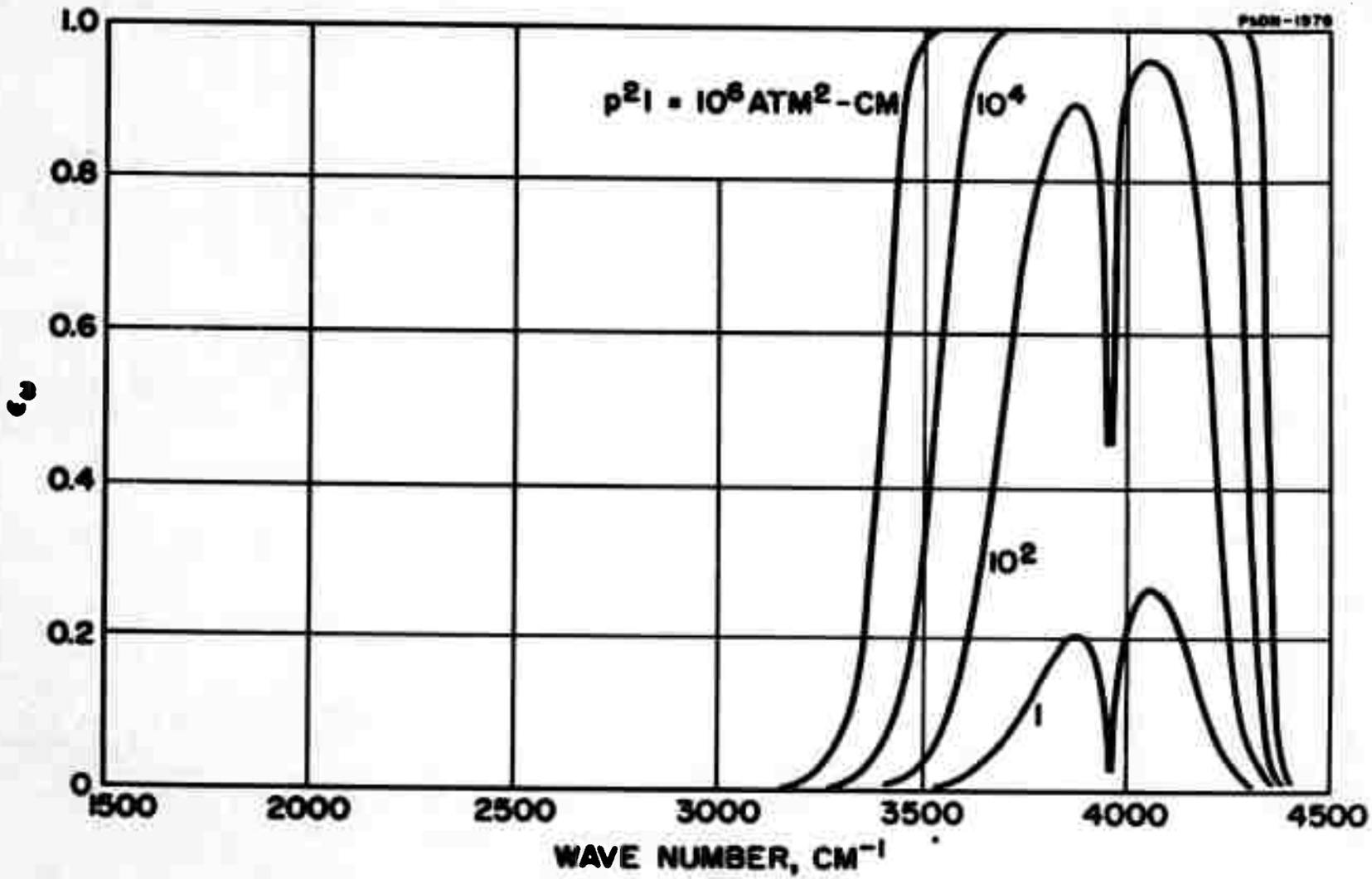

FIGURE 25 SPECTRAL EMISSIVITY OF HF AT T=300°K
(STRONG LINE APPROXIMATION)

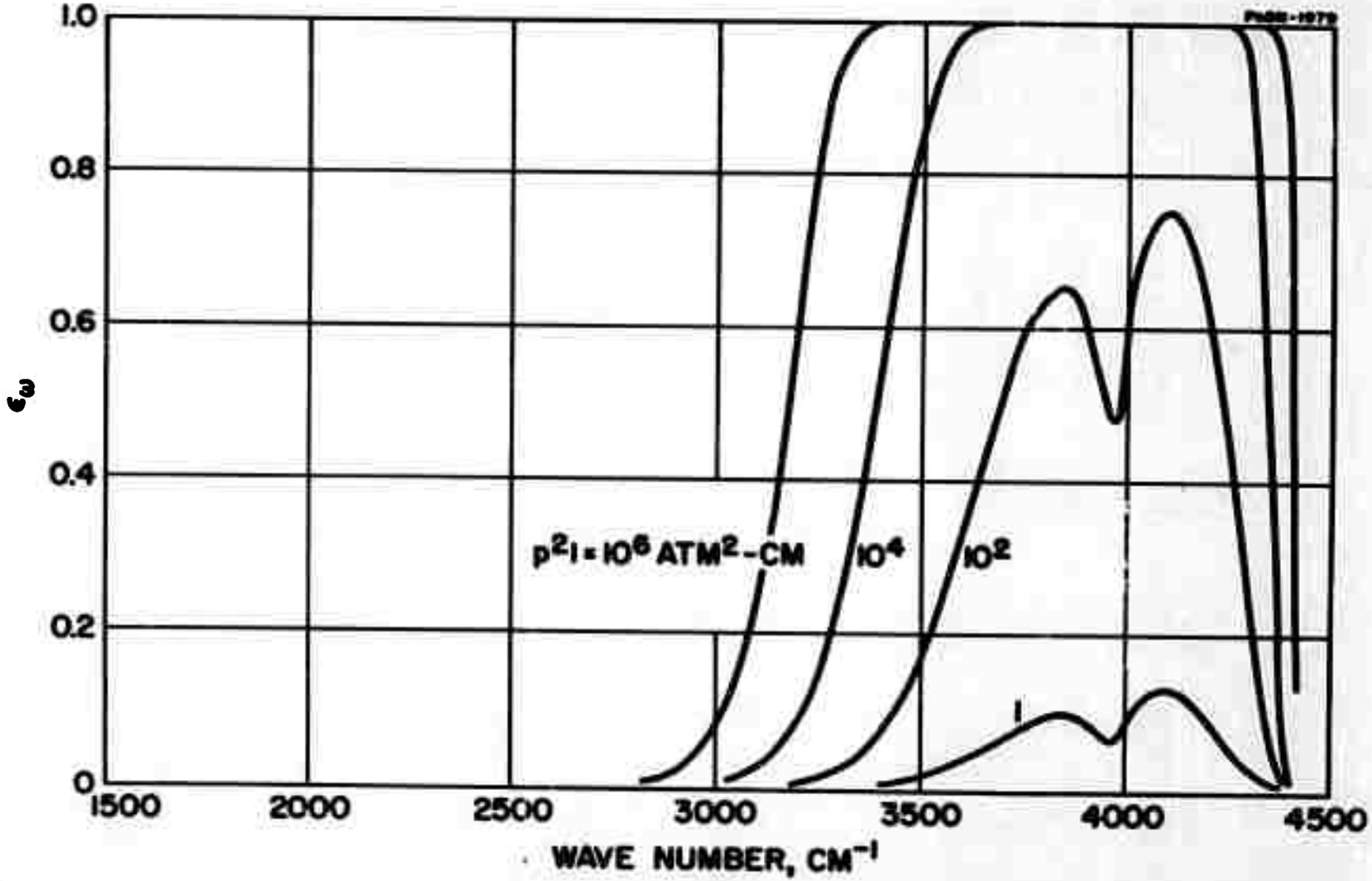

FIGURE 26 SPECTRAL EMISSIVITY OF HF AT T=600°K
(STRONG LINE APPROXIMATION)

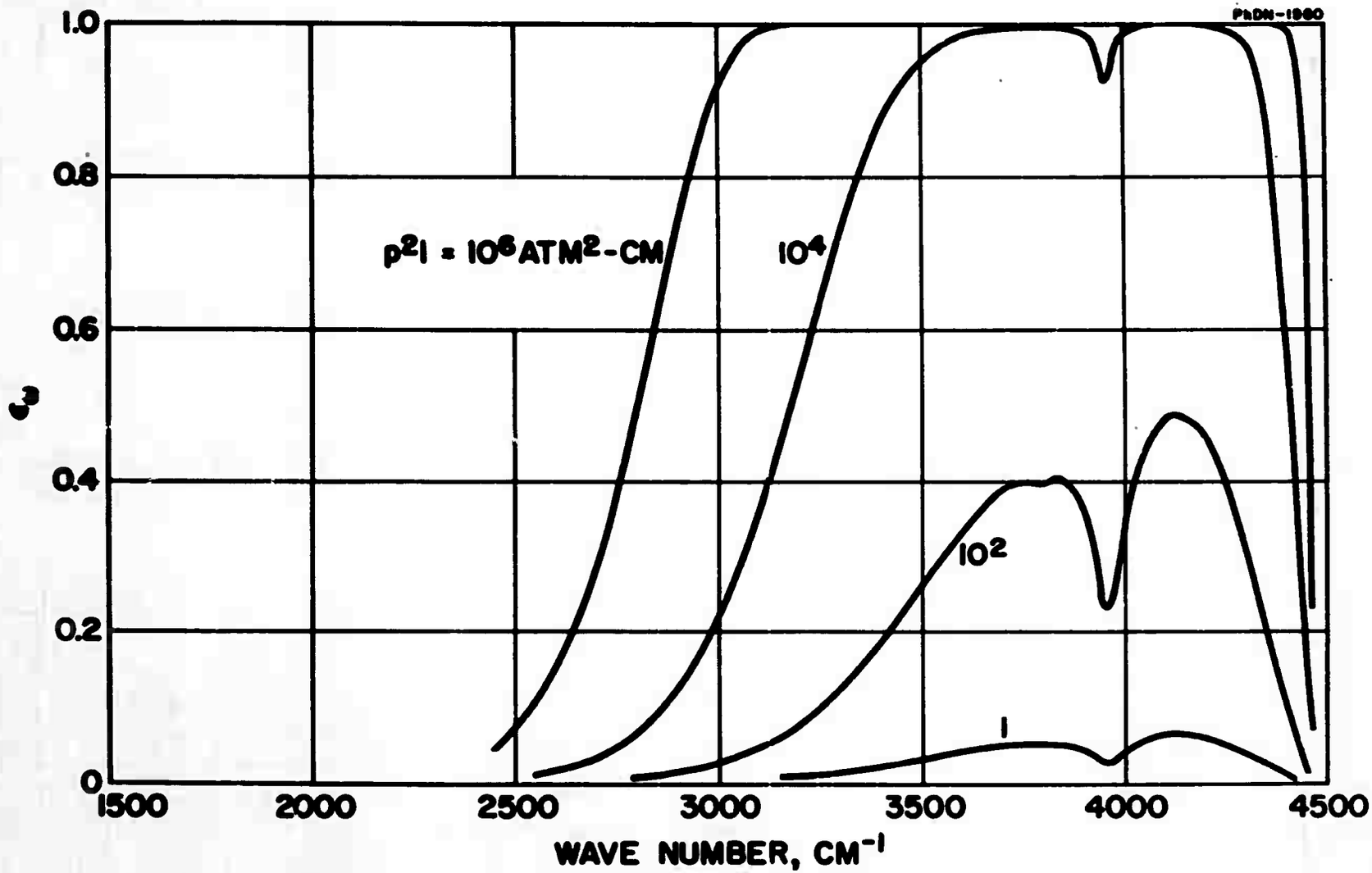

FIGURE 27 SPECTRAL EMISSIVITY OF HF AT T=1200°K
(STRONG LINE APPROXIMATION)

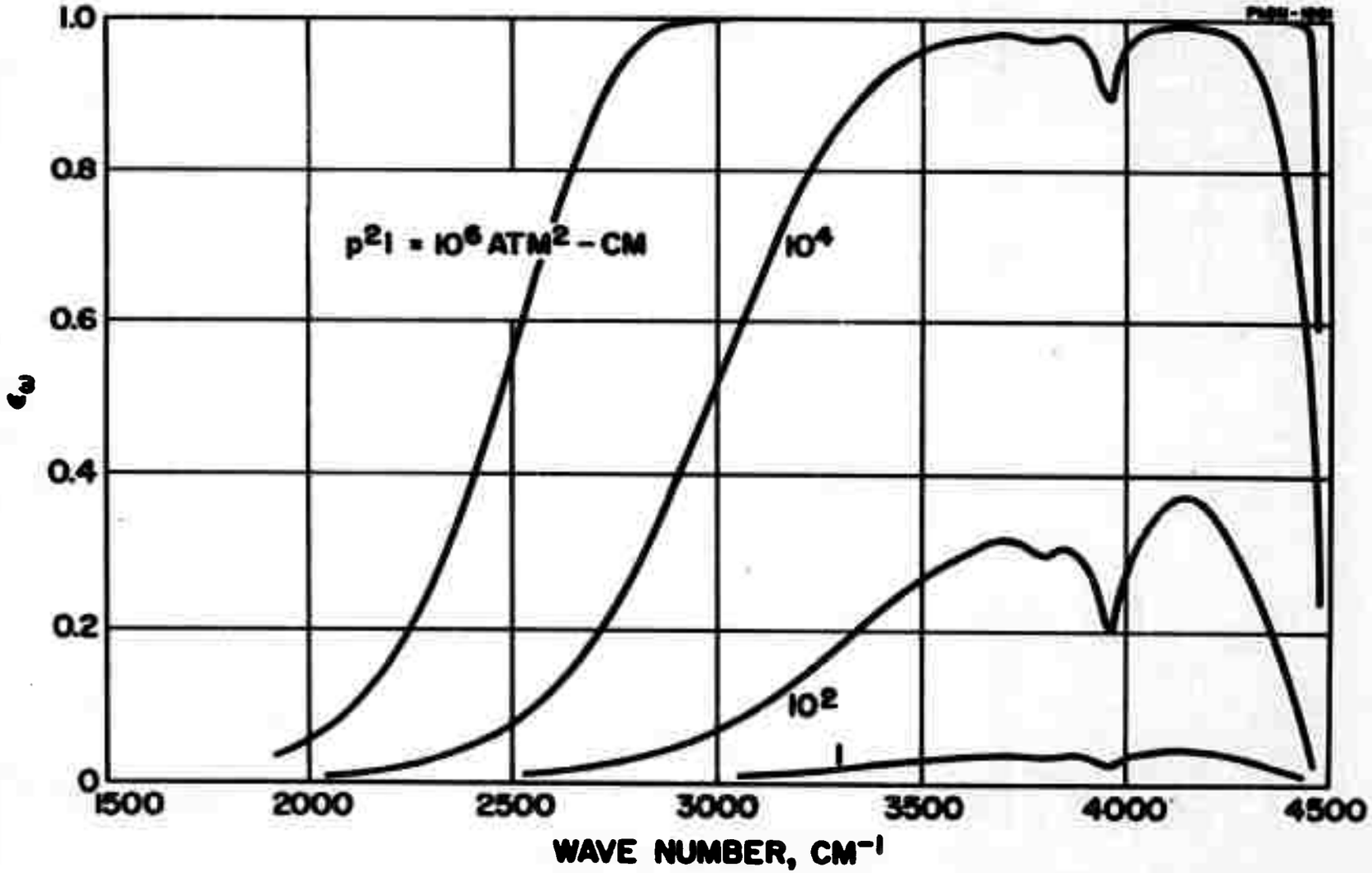

FIGURE 28 SPECTRAL EMISSIVITY OF HF AT T = 1800°K
(STRONG LINE APPROXIMATION)

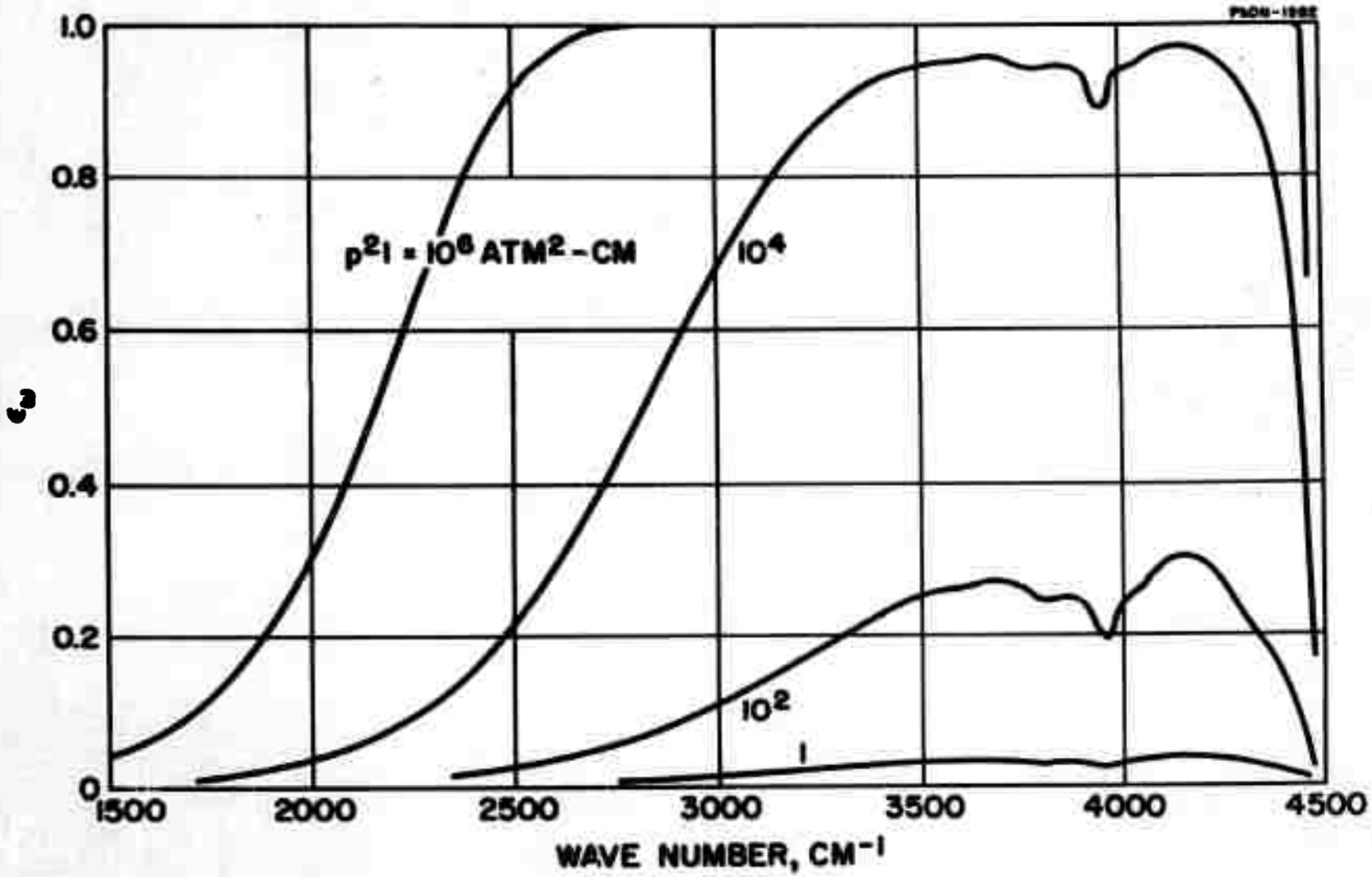

FIGURE 29 SPECTRAL EMISSIVITY OF HF AT T=2400°K (STRONG LINE APPROXIMATION)

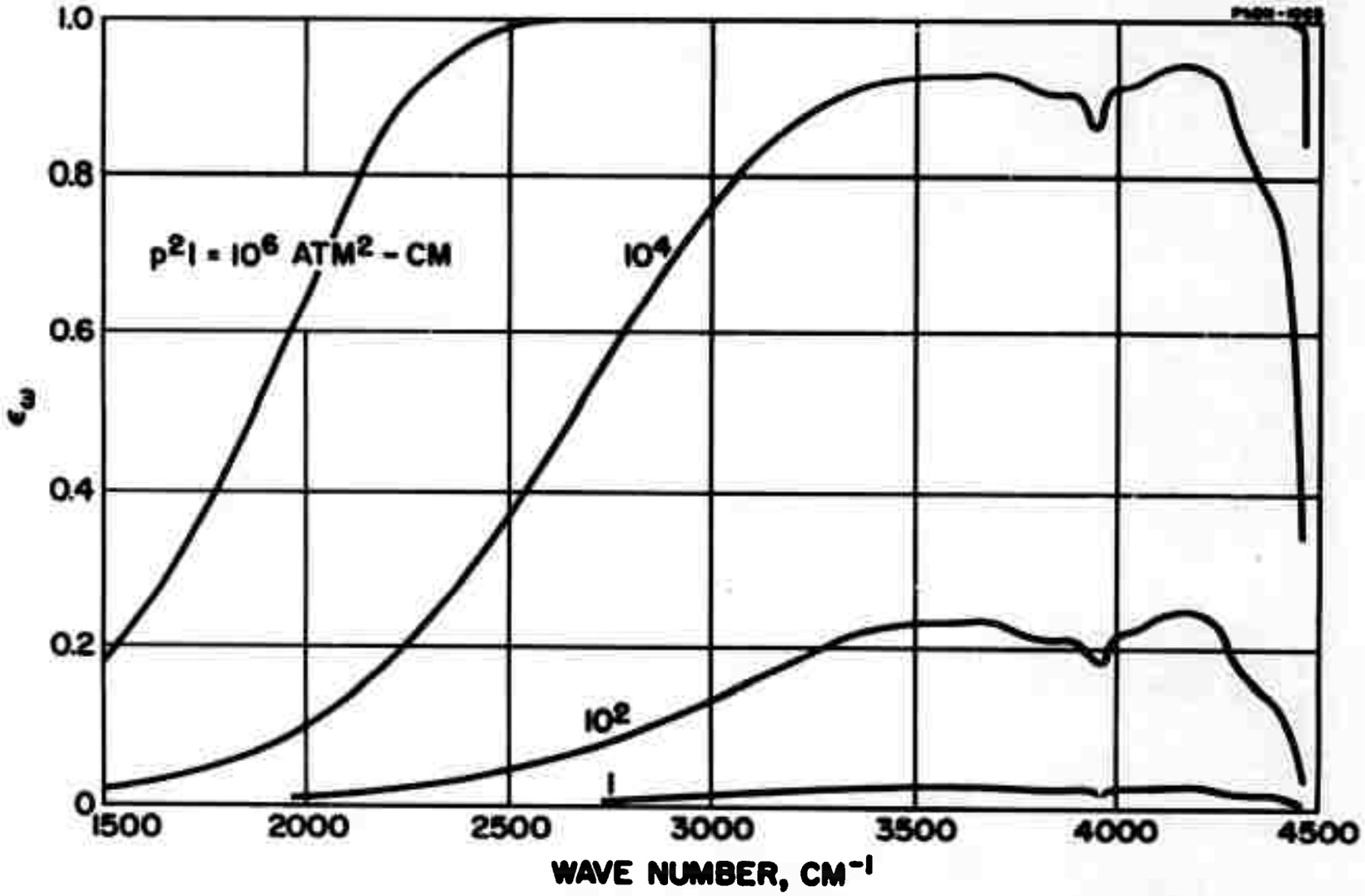

FIGURE 30 SPECTRAL EMISSIVITY OF HF AT T = 3000°K
(STRONG LINE APPROXIMATION)

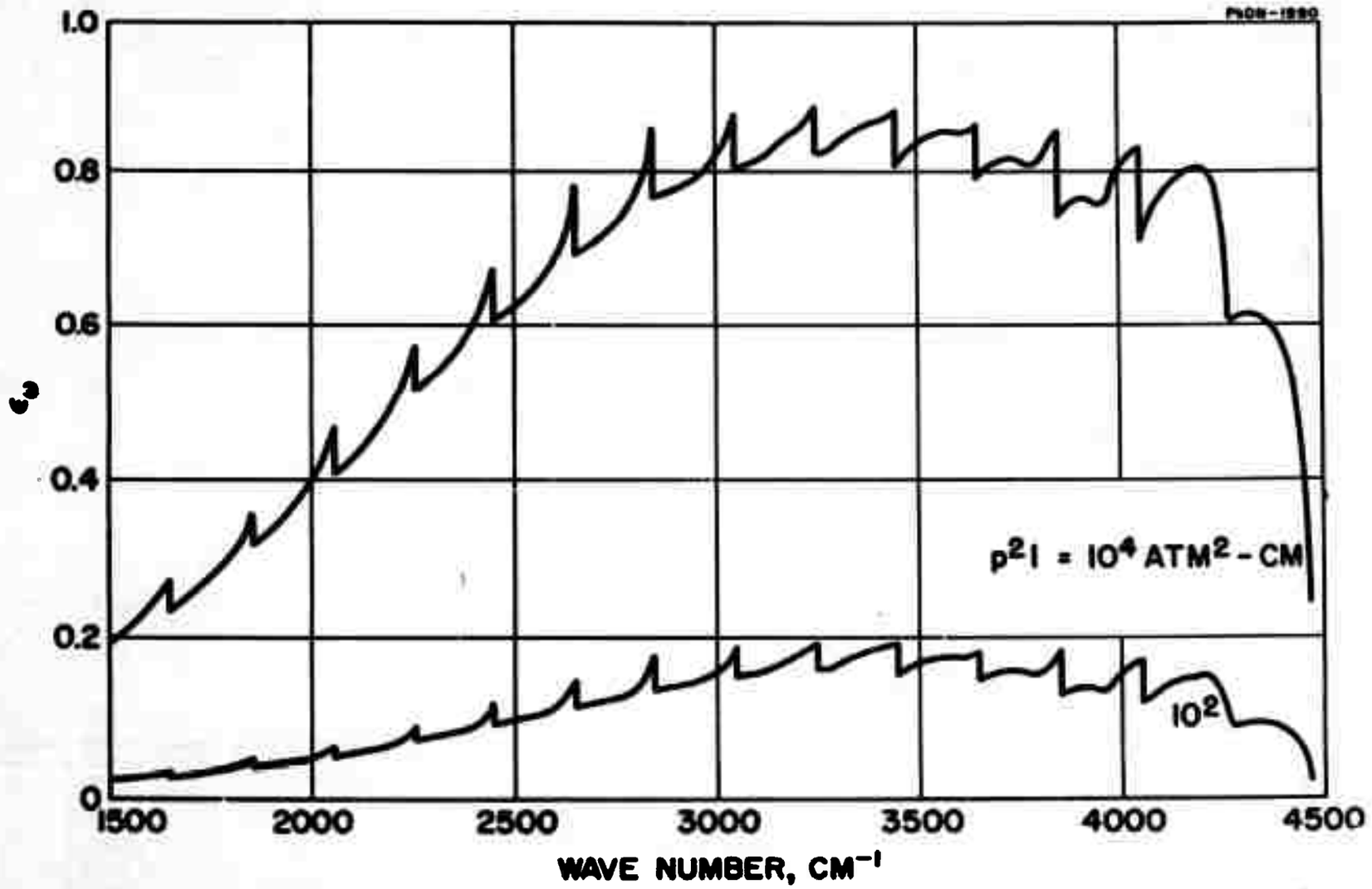

FIGURE 31 SPECTRAL EMISSIVITY OF HF AT T=5000°K
(STRONG LINE APPROXIMATION)

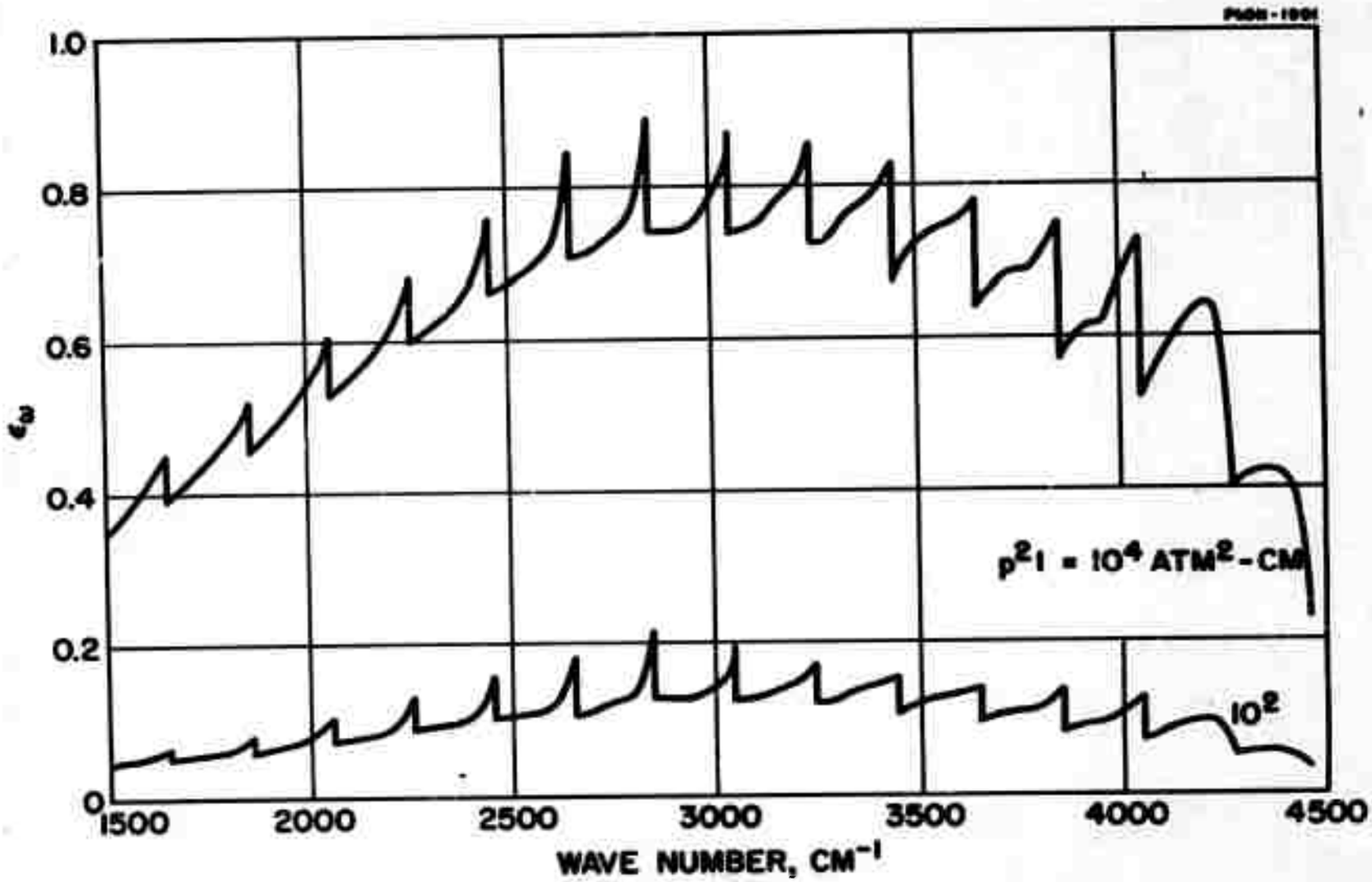

FIGURE 32 SPECTRAL EMISSIVITY OF HF AT T=7000°K (STRONG LINE APPROXIMATION)

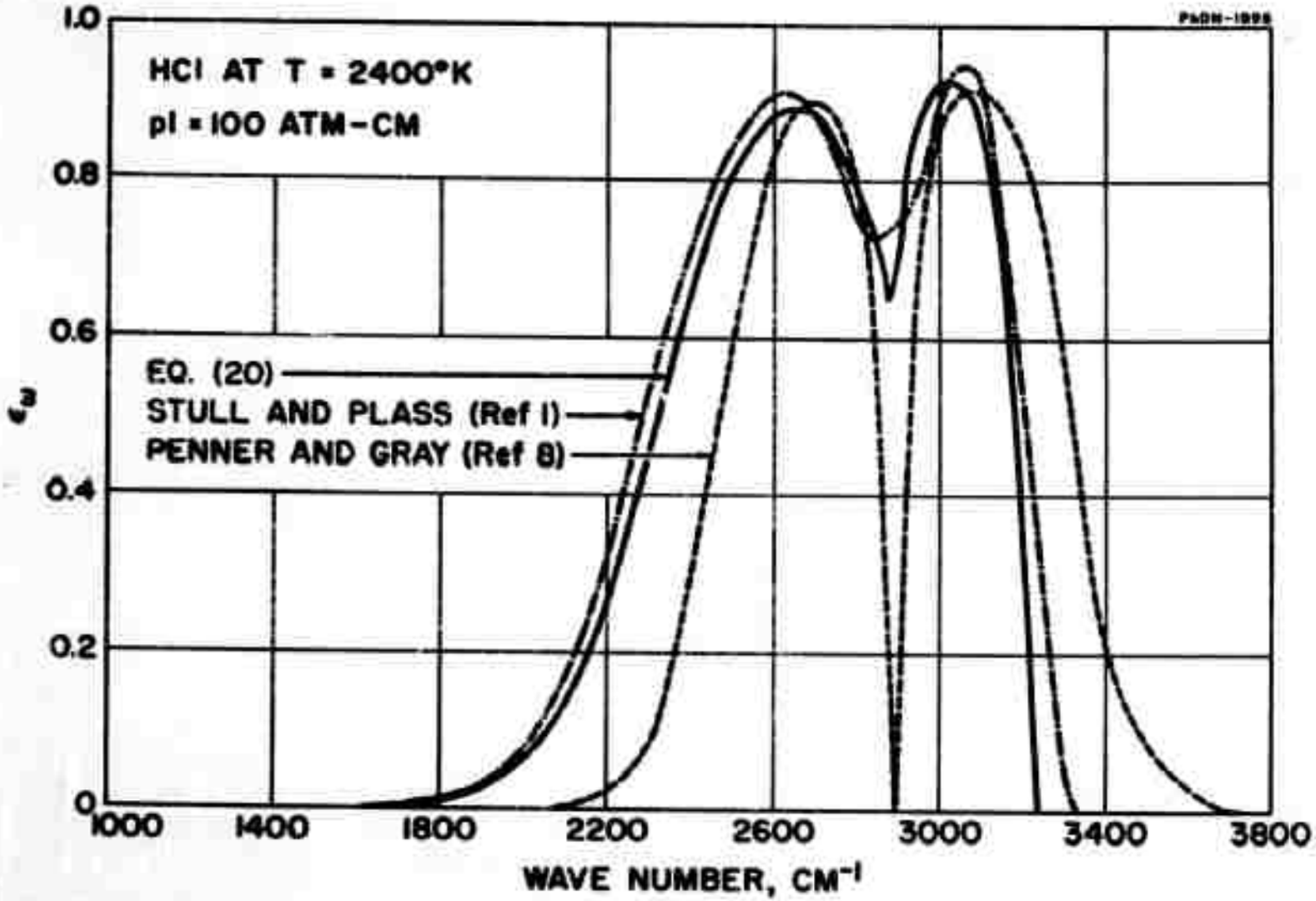

FIGURE 33 COMPARISON WITH OTHER PUBLISHED DATA OF SPECTRAL EMISSIVITY COMPUTED FOR HCℓ AT T=2400°K IN THE WEAK LINE APPROXIMATION

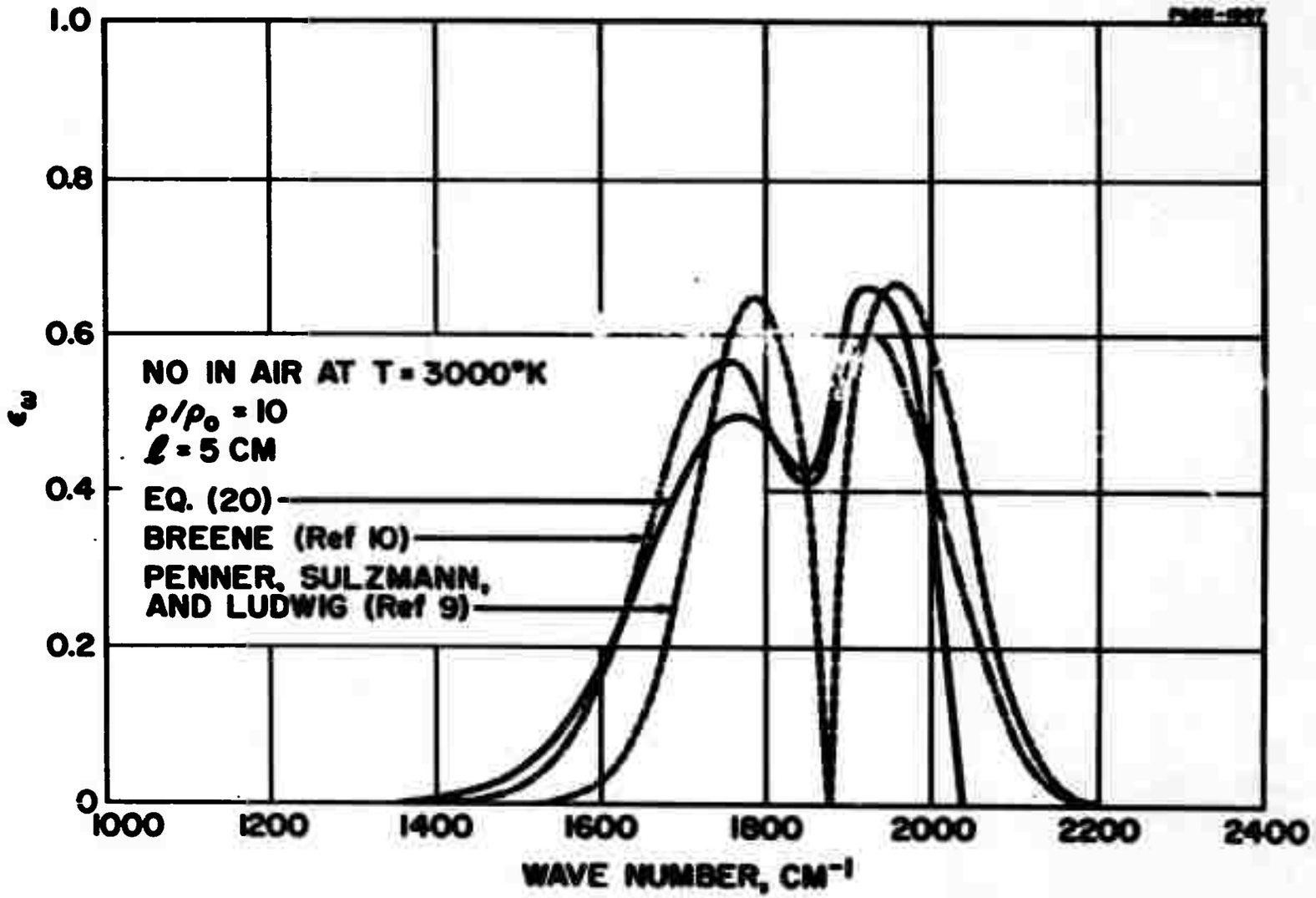

FIGURE 34 COMPARISON WITH OTHER PUBLISHED DATA OF SPECTRAL EMISSIVITY COMPUTED FOR NO AT T=3000°K IN THE WEAK LINE APPROXIMATION

if the previously mentioned correction for line wing emission beyond the band head had been included in this analysis. Presumably the tail drawn by Stull and Plass[1] in the region near 3300 cm^{-1} was computed for one particular combination of path length and pressure, perhaps for p = 100 atm and ℓ = 1 cm.

Figure 34 shows the results of a computation by Breene[10] (for NO in air at 3000°K, density ratio = 10, thickness = 5 cm). Penner, Sulzmann, and Ludwig's[9] results for the simple harmonic oscillator model are also shown. It should be noted that for comparison all three of these computations utilized Breene's[10] multiplicative factor of 1.88 for the average path length (i.e., for a 5-cm-thick layer, a value of ℓ = 9.4 cm was used).

A glance at Figure 34 shows that Equation (20) is not much more successful than the simple harmonic oscillator approximation in matching Breene's[10] computation. The correction for line wing emission would add a tail to the curve representing Equation (20) and extend it somewhat farther past 2000 cm^{-1}. (Since the line widths are of the order of 2 cm^{-1}, this addition would not be very significant.) The highly asymmetric peaks in emissivity indicated by Equation (20) seem more reasonable than the nearly symmetric peaks shown by Breene.[10] (Note, in comparison, that for HCl, the inclusion of the Herman and Wallis[11] F-factor has caused a considerable augmentation of emissivity at lower frequencies and diminution at higher frequencies which makes the peaks nearly equal. This factor is negligible for the more symmetric NO molecule so that considerably more asymmetry would be expected on this basis.)

Emissivities have been computed (but not presented here) for HCl and HF in the weak line approximation and for CO and NO in the strong line approximation for the temperatures considered here. Also for several intermediate temperatures, emissivities have been computed for all four molecules in both approximations. It is planned to extend the computations to other molecules and also to consider Doppler broadening as well as Lorentz broadening.

REFERENCES

1. V. R. Stull and G. N. Plass, J. Opt. Soc. Am. 50, 1279 (1960).
2. G. N. Plass, J. Opt. Soc. Am. 50, 868 (1960).
3. W. S. Benedict, R. Herman, G. E. Moore, and S. Silverman, Can. J. Phys. 34, 850 (1956).
4. H. Babrov, G. Ameer, and W. Benesch, J. Mol. Spectroscopy 3, 185 (1959).
5. D. Weber and S. S. Penner, J. Chem. Phys. 21, 1503 (1953).
6. W. S. Benedict and E. K. Plyler, "High-Resolution Spectra of Hydrocarbon Flames," in Energy Transfer in Hot Gases, pp. 57-73, N. B. S. Circular No. 523, Washington, D. C., 1954.
7. G. A. Kuipers, J. Mol. Spectroscopy 2, 75 (1958).
8. S. S. Penner and L. D. Gray, J. Opt. Soc. Am. 51, 460 (1961).
9. S. S. Penner, K. G. P. Sulzmann, and C. B. Ludwig, Convair Report ZPh-079, November 29, 1960.
10. R. G. Breene, Jr., J. Chem. Phys. 29, 512 (1958).
11. R. Herman and R. F. Wallis, J. Chem. Phys. 23, 637 (1955).

UNCLASSIFIED

UNCLASSIFIED